C.P. No. 1320

C.P. No. 1320

PROCUREMENT EXECUTIVE, MINISTRY OF DEFENCE

AERONAUTICAL RESEARCH COUNCIL

CURRENT PAPERS

The Characteristics of a Family of Rooftop Aerofoils Designed at their Drag-Rise Condition in Viscous, Compressible Flow Part 1: Design Condition

by

B. G. J. Thompson and S. W. Cosby

LONDON: HER MAJESTY'S STATIONERY OFFICE

1975

PRICE £1-80 NET

UDC 533.692 : 533.6.048.2 : 533.6.013.12 : 532.526.5

**CP No.1320
July 1972

THE CHARACTERISTICS OF A FAMILY OF ROOFTOP AEROFOILS DESIGNED AT THEIR DRAG-RISE CONDITION IN VISCOUS, COMPRESSIBLE FLOW

Part 1: Design condition

by

B. G. J. Thompson
S. W. Cosby*

SUMMARY

Twenty-eight members of the original family of aerofoils, presented in TDM 67010 [3], have been redesigned using an inverse method which takes account of the major influence of the boundary layer and wake on the pressure distribution. The more accurate compressibility law devised by Wilby and Lock is used. Hodges[9] results suggesting that the published family has an overoptimistic performance are confirmed. The new sections have design lift coefficients which are usually lower than the original values by amounts up to 10%. Their drag coefficients are higher by 0.0001 to 0.0004 but they have a wider range of attached flow in conditions of practical interest, according to Stratford's method, because of more realistic trailing edge pressures.

The drag values, separation boundaries and drag-rise boundaries are presented in Ref.12, together with tabulation of ordinates and design pressure distributions for the complete series of redesigned aerofoils. The present Report considers mainly the 50% rooftop sections as typical examples and discusses the basis upon which the new designs were obtained.

---

* Aerodynamicist, Short Brothers and Harland Ltd., Belfast.

** Replaces RAE Technical Report 72141 - ARC 34 437.

CONTENTS

1 INTRODUCTION

Until comparatively recently, aerofoils for transonic cruise conditions were often designed by using NACA camber and thickness forms[1] as a starting point. The original family of aerofoils presented in Refs.2 and 3, was chosen to provide a rather better datum series from which the aircraft designer could develop suitable sections for his particular purpose. An aerodynamic specification*, in the form of a prescribed upper-surface pressure distribution at design conditions, was chosen as shown in Fig.1. This was characterised by a flat rooftop of length x_R/c** followed by a linear pressure recovery to a plausible trailing edge value. The rooftop level was such that the local Mach number at, and ahead of, the aerofoil crest, was 1.02 ($p/H_0 = 0.515$). According to the empirical theory of Sinnott[2] this ensured that the aerofoil carried the maximum possible lift at design condition, for a given design Mach number (M_{des}) and thickness form, without incurring any wave-drag penalty. The off-design behaviour, with increase of either Mach number or C_L, would also be favourable in that a hollow leading-edge suction loop resulted which (again empirically) avoids any premature drag 'creep'[2]. Two additional advantages of the original (TDM) specification were:

(a) the small number of design variables which enable exchange rates to be readily assessed and presented as a guide to the designer, and

(b) that the predicted performance of the aerofoils (which could be designed using prediction methods for subcritical flow) was superior to that of conventional NACA sections.

Although with the introduction of further degrees of freedom in the design - such as a supercritical leading-edge velocity peak, or increased loading near the trailing edge - the performance of modern aerofoils is now generally higher than the TDM series, nevertheless the series remains the only coherent datum family and has overall characteristics which are only slightly inferior to the latest sections and which in any case could not be designed directly by existing theoretical procedures.

---

* Henceforth referred to for the sake of brevity as the 'TDM specification'.

** The thickness form associated with a given pressure distribution need not have the same rooftop length but for simplicity this was chosen for the TDM family. Thus, for example an RAE 102 form is always used with a 40% rooftop, RAE 103 with 50%, and so on.

The original family of rooftop aerofoils was designed using an inverse version of the RAE standard method[4] (two-dimensional) with the Wilby[5] compressibility factor applied to thickness terms only. Profile drag coefficients, for the upper and lower surfaces, at the rooftop design condition $\left(C_{L_{des}} = C_{L_D}, M_{des} = M_D\right)$ were predicted using Nash's method[6,22]. Charts were presented in Ref.13, in carpet form, for the variation of drag coefficient with chord Reynolds numbers (R_c) in the range 10^6 to 10^8 and with transition positions (x_{tr}/c) in the range 0 to x_R/c. Each chart was necessarily confined to those sections with given M_{des} and x_R/c having a maximum range of thickness/chord ratios from 0.06 to 0.18.

Comparisons with the nominally exact results of Sells[7] have shown that the use of Ref.5 in its original form underestimates the effect of compressibility on the lifting terms, whereas the more recent formula due to Lock, *et al.*[8] gives reasonably good results for sections of the present type. This applies to both design and off-design conditions provided the latter remain nominally subcritical, although small supercritical peaks near the leading edge can usually be predicted with sufficient accuracy for present purposes. Hodges[9] considered the 102 series which has 40% rooftops and showed that, as a result of the change in compressibility correction, the values of design lift coefficient $C_{L_{des}}$ associated with any given TDM specification $(M_D, t/c, x_R/c)$ had been overestimated by amounts varying from 0 to 10% depending upon the thickness/chord ratio.

From a practical point of view, the original design performance can be recovered by a reduction of about 1% in t/c, at a given x_R/c. Using a slightly revised wake law in the Nash drag calculation he showed also that the upper-surface drag was very slightly larger or the same as before, whilst the lower-surface values were increased by the larger adverse pressure gradients resulting from the revised pressure calculations. This meant that, for a given M_{des} and t/c, the drag coefficient at design $\left(C_{D_{des}}\right)$ was raised by between 2% and 6% and, combined with the lower values of $C_{L_{des}}$, resulted in appreciable reductions in lift/drag ratio, $C_{L_{des}}/C_{D_{des}}$, for example. At a given $\left(C_{L_{des}}, M_{des}\right)$ the lower t/c apparently gave no reduction in $C_{D_{des}}$ compared with the published family, however.

Neither the new calculations nor the original TDM predictions allowed for the proper interaction between the viscous and the inviscid parts of the calculation. Consequently the trailing edge pressures, for example, were incorrectly assumed to be independent of Reynolds number and of transition position. This interaction would change the pressure gradient on the upper surface and hence the predicted rear separation boundaries, as well as further modifying the distribution of drag between separate surfaces, although the total drag itself might not be very strongly affected.

The viscous/inviscid interaction is accounted for adequately for present purposes by the iterative method of Powell[7,10,11] provided comparison with measurement is made at a given C_L. The availability of a matched pair of forward and inverse design programs* and the experience accumulated at Teddington in a number of design exercises during recent years led the Ministry of Technology/Industry Drag Analysis Panel to propose that these programs should be used to redesign a number of sections and to evaluate new drag charts to replace the existing (overoptimistic) values as these latter might mislead the designer seriously if not updated soon. Subsequently a contract** was issued to the Aerodynamics Department of Short Brothers and Harland, Belfast to carry out these design point computations and to evaluate possible forms of presentation. In addition, the contract made provision for a limited amount of computing time for drag calculations in off-design conditions, and the recalculation of rear separation boundaries.

This Report discusses, in section 2, the basis of the design method used and goes on, in section 3, to describe a number of preliminary calculations carried out at Teddington to investigate practical questions concerning the choice of sections and the values of transition positions etc. that were to be used in the body of computations to be made at Belfast. All the inverse designs were carried out at Teddington. Their overall characteristics are summarized here but the complete set of results is presented in the final contract report[12] for the design condition. These results are discussed here selectively and it is confirmed that the new values of $C_{L_{des}}$ are reduced by as much as 10% (see, for example, Fig.15) and the values of drag are generally higher for a given specification (M_{des}, t/c, x_R/c) by as much as 5%. Fig.21 shows a typical carpet of Ref.13 compared with the new results.

---

* RAE (Teddington) programs;
JWDØBP5 -- and JWBTBP3 -- in KDF9 ALGOL.

** Ministry of Technology Contract K5D/08/CB5DAR.

The effect of varying R_c and transition position on trailing edge pressure coefficient is compared with the unique value supposed earlier (see Fig.23) and the large changes this implies in terms of the separation boundary in the Reynolds number *versus* transition position plane is shown in Fig.24.

Relationships have been obtained between the new values of drag and the original values. A typical example, from Ref.12, is given here as Fig.19 for the 50% rooftop sections. It is found that the differences in C_{D_u}, C_{D_ℓ} and total C_D, between the corresponding sections from the original and the new families, can be plotted in a very simple carpet form shown here as Fig.20. These relationships seem to be independent of R_c, t/c and x_{tr}/c.

Consequently, whilst it is thought essential to replace the original TDM presentations of design point loci $C_{L_{des}}$ *versus* M_{des}* and of section ordinates, it would be wasteful to replace the original profile drag charts. Instead, only the figures showing the differences in drag are needed together with some explanation in the form of typical correlations of the kind shown here as Fig.20.

If the new drag carpets are required for any purpose then these are presented in Ref.12.

Seven aerofoils from the new family have been selected as a basis for computations in off-design conditions and a description of this work is given in a companion paper[14].

2 THE METHOD OF PREDICTING AEROFOIL SHAPES, PRESSURE DISTRIBUTIONS AND PROFILE DRAG VALUES IN ATTACHED, SUBCRITICAL COMPRESSIBLE, VISCOUS FLOW

2.1 The aerofoil design method

The method of prediction, described in Ref.10, iterates between pressure and boundary-layer calculations. The pressure calculation, at any stage, assumes an inviscid flow about the current estimate of the displacement surface formed by the aerofoil, boundary layer, and wake. The calculation of the boundary-layer displacement thickness is based upon the pressures found as a result of the preceding iterations.

The Weber[15] method for pressure prediction is used with the semi-empirical compressibility law devised by Lock, *et al.*[8]. Wake curvature is not considered but an analytic approximation to wake thickness is employed.

---

* By a series of figures similar to Fig.15, for example.

The turbulent boundary layer is predicted using the local equilibrium method of Nash[6] whilst the calculation of laminar flow is based on Thwaites' procedure[16] together with the compressibility transformation of Rott[17].

The inverse (design) program calculates the camber ordinates, incidence and lower-surface pressures once the thickness form and desired upper-surface pressures are specified. The iterative calculation includes an adjustment of these pressures to permit the thickness of the displacement surface at the trailing edge to be compatible with the pressure predicted there. This adjustment takes the form of a linear variation to the trailing edge from the Weber point nearest to the end of the rooftop, thus retaining the 'TDM specification' of a linear pressure rise to the trailing edge.

Firmin[18], has recently produced a prediction method for aerofoil behaviour in viscous, compressible flow, which represents an advance over the Powell method. The vorticity in the wake is accounted for using a method analogous to that employed by Spence[19] for the thin aerofoil jet flap, and the boundary-layer and wake-displacement thicknesses are found from the Green/Head entrainment approach[20]. This results in more reliable predictions for the pressures in the immediate vicinity of the trailing edge but as yet there is little experience of its usefulness for drag prediction.

A comparison between the present method, and that of Firmin is given, for the 40% rooftop aerofoil 102-10-40-70 at design condition, in Fig.2. Excellent agreement for the pressure distributions is obtained provided the same C_L is used in both calculations. The profile drag values differ by less than 2% and this also may be considered to be very satisfactory.

2.2 Profile drag prediction

Once the aerofoil calculation has converged the drag is found from the momentum thickness at the trailing edge by using a wake relationship of the Squire-Young[21] type. Nash introduced changes in the exponents of the compressible flow version in order to match the observed variation of C_D with Mach number (i.e. drag 'creep'). He also assumed that if the value of R_θ, at transition, was less than 320 then the initial value for the turbulent boundary-layer calculation should be raised to this value*.

Several detailed discussions of the drag and boundary-layer methods of Nash have been presented by the Engineering Sciences Data Unit of the

---

* This is only likely to affect results at very low chord Reynolds numbers around 10^6. There is physical justification for this assumption only in zero pressure gradient, incompressible flow.

Royal Aeronautical Society. Ref.22 considers the wake law, Ref.23 the prediction of separation and comparison with Stratford's method (see Ref.1), whilst the assumptions for transition and the effect of trailing edge pressures on drag are considered in Refs.24 and 25, respectively.

Conventional assessments of the accuracy of a prediction method for profile drag depend essentially on comparison with nominally two-dimensional wind-tunnel experiments. Thus the problem is not purely one of turbulent boundary-layer (and wake) prediction, but depends also upon a knowledge of the position and nature of transition and on the degree of two-dimensionality actually achieved in the tests[27]. The span/chord ratios of models commonly used in aerofoil testing facilities are small* and the shape of the displacement surface of the interaction region between the sidewall boundary layer and the aerofoil will depend on model attitude, thickness and lift coefficient. The displacement effect, and hence the amount of flow convergence induced at the centre plane of the model, will depend also on the characteristics of the sidewall boundary layer itself. Other three-dimensional features are present in standard test procedures (see Ref.27 for further details).

In view of the large number of factors that might affect comparisons between theory and experiment it has always been assumed that the overall level of possible disagreement had a random behaviour. Consequently, a body of such data was employed to calibrate and test predictive methods of the simple empirical type used here and it was claimed that the overall level of agreement with experiment was about ±2%. Such very simple reasoning was thought to be preferable, in order to obtain comparative results for families of aerofoils tested in a given tunnel, to the alternative of waiting for the results of basic experiments which might lead to the prediction of transition behaviour or to a proper treatment of departures from the simple two-dimensional flow assumed in the calculations.

Now, although such arguments are unsatisfactory from a fundamental point of view, it has been difficult in the past to distinguish clear trends of systematic disagreement between the Nash prediction method (used here) and experiment.

As a striking example of this, the comparisons available for tests conducted in the Teddington 20in × 8in tunnel have been taken. The percentage differences between theory and experiment are plotted, in Fig.3, as a function

* About 1.5 in small British transonic wind tunnels for which the body of profile drag data are available, and as low as 0.42 in some older NACA tests, quoted by Osborne[26].

of C_L. The large degree of scatter as C_L exceeds 0.5 is readily apparent and it is difficult to apply, with confidence, any rigorous statistical examination of these results even on the hypothesis that there is 'no correlation with C_L', as the exact weighting to be applied to each plotted point is very uncertain. For example, systematic effects will probably be present because only the sections with the larger C_L values have rear loading.

Transition 'position' has been found by the examination of shadow photographs and it is convenient to assume that this is the major source of (random) uncertainty. It is very difficult, especially for the lower surface of a lifting aerofoil at the lower Mach numbers, to obtain a clear indication of changes in boundary-layer profile properties. Other techniques for detecting transition are unsuitable for routine test purposes, unfortunately.

One of the aerofoils considered in Fig.3 is RAE (NPL) 3111 which has a 35% flat sonic rooftop at its design condition and is very similar in specification to a member of the aerofoil family designed here. In Figs.4 and 5 direct comparisons of measured and predicted profile drag values are made over a range of C_L, at a constant Mach number, for this section. The data shown in Fig.4 are taken from the 20in × 8in tunnel and this figure is merely an alternative presentation of some of the results already seen in Fig.3. In Fig.5, however, the data are taken from the more reliable experiment conducted in the RAE 8ft wind tunnel at much higher Reynolds numbers.

The span/chord ratio of the model was 3.2 in this case compared with 1.6 in the Teddington tests. The comparison in Fig.5 is a demonstration of the usefulness of the present simple method both in design and in off-design conditions. The disagreement between theory and experiment is no larger than the difference between the wake traverse and balance drags themselves.

Once an effective transition position is *defined* and the flow is also *defined* to be two-dimensional then the prediction of drag is likely to be reliable because it depends principally upon the solution of the first-order momentum integral equation. The latter can only be in error close to the trailing edge and, as explained by Thompson, *et al.*[27], as the pressure gradients behind the trailing edge are roughly equal and opposite in sign to those immediately ahead of the trailing edge, local departures from the boundary-layer approximation should cancel so that well downstream ($x/c > 1.5$, say) the momentum loss will be accurately predicted. Even the relatively crude method used here will therefore be as reliable as any individual drag measurement and

more consistent and reliable as a guide to exchange rates (with M or C_L) than the results from many aerofoil testing facilities. An exception to this may be when appreciable rear loading is present, which is not the case for the family of aerofoils considered here.

2.3 Rear separation

Two alternative separation predictions have been used in the past, namely Stratford's method in a form suitable for compressible flow[2] and the assumption that the pressure-gradient parameter π, appearing in the local equilibrium calculation, takes a value of 10^4 at separation. Ref.23 indicates that these methods give good agreement for a truly linear pressure rise as on the earlier aerofoils.

However, reference to Fig.6 for the new calculations with section 103-14-50-70 shows a less satisfactory correlation between any chosen value of π and the Stratford result. This may be caused by the local departure (see Fig.12, for example) near the trailing edge, of the upper-surface pressures from a truly linear form when the new section is run at Reynolds numbers or with transition positions other than those used in the inverse calculation. This is a disadvantage of the Nash method.

Consequently, the present investigation used Stratford's method, on the 'equivalent' linear pressure rise from end of rooftop to $[C_p]_{te}$ ignoring any concavity or convexity of the actual pressure distribution. This had the advantage of being consistent with the existing work of Ref.2.

Some definition of 'significant' separation from a practical point of view is clearly required as the results in Fig.7 indicate. These show the variation of boundary-layer properties, H, π, C_f and G, at the trailing edge of 103-10-50-70, over a range of incidence at $M = 0.65$.

If separation is assumed, for instance, to occur at $\pi = 100$ then this has started even at design incidence ($\alpha = \alpha_D = 2.04^\circ$), but if $\pi = 1000$ then the section can run up to 5° without separation, whilst α can rise to 6.5° if $\pi = 10^4$ is chosen.

This represents a very large uncertainty in C_L over which it should be noticed H lies between 2.5 and 3.0. These values have all been thought to be reasonable separation criteria in the past.

3 DESIGN POINT CALCULATIONS

3.1 Preliminary work

A number of questions had to be answered before the new family of sections could be designed and the main programme of computing could be undertaken to prepare the new drag charts. Calculations were made on sections 103-10-50-70 and 103-14-50-70.

3.1.1 The choice of section design point in the presence of viscous effects

For each design point, specified by M_{des}, t/c and x_R/c, the section resulting from the inverse program will have a camber shape and incidence that will depend upon the assumed transition positions and the Reynolds number. It was obviously undesirable to have a different section for each of these combinations and so an inverse design condition was required to produce a suitable 'mean' section for each combination of M_{des}, t/c and x_R/c corresponding to a particular member of the original aerofoil family and having a unique value of design C_{L_D}, for example. The drag values and separation boundaries could then be worked out for each of these 'mean' aerofoils as a function of R_c and transition position.

As the Reynolds number is reduced, or the transition position moves forward (on the upper surface especially) the thickness effect due to the viscous displacement surface increases at the trailing edge. This causes a progressive departure from the mean pressure distribution assumed earlier[2] in extrapolating linearly to the trailing edge. The thickness pressures will fall and if the inverse procedure is to achieve the desired linear pressure variation on the upper surface it must remove this trend towards a concave pressure distribution at low Reynolds numbers by adding extra rear camber; compare the camber lines shown in Fig.8 for nominally the same TDM specification 103-14-50-70 but assuming very different R_c values (10^6 and 10^8). Consequently a progressive increase of rear loading occurs with reduction of Reynolds number (Fig.9). A similar but less severe effect is produced by forward movement of transition (Fig.10).

This is admittedly a fairly severe case as there is a mild rear separation predicted for $R_c = 10^6$ and $x_{tr}/c \leq 0.25$ on the upper surface, but even a change from 10^8 to 10^7 (where the flow is completely attached) for $x_{tr}/c = 0.05$, as Fig.9 shows, leads to a difference in C_{L_D} of nearly 5%.

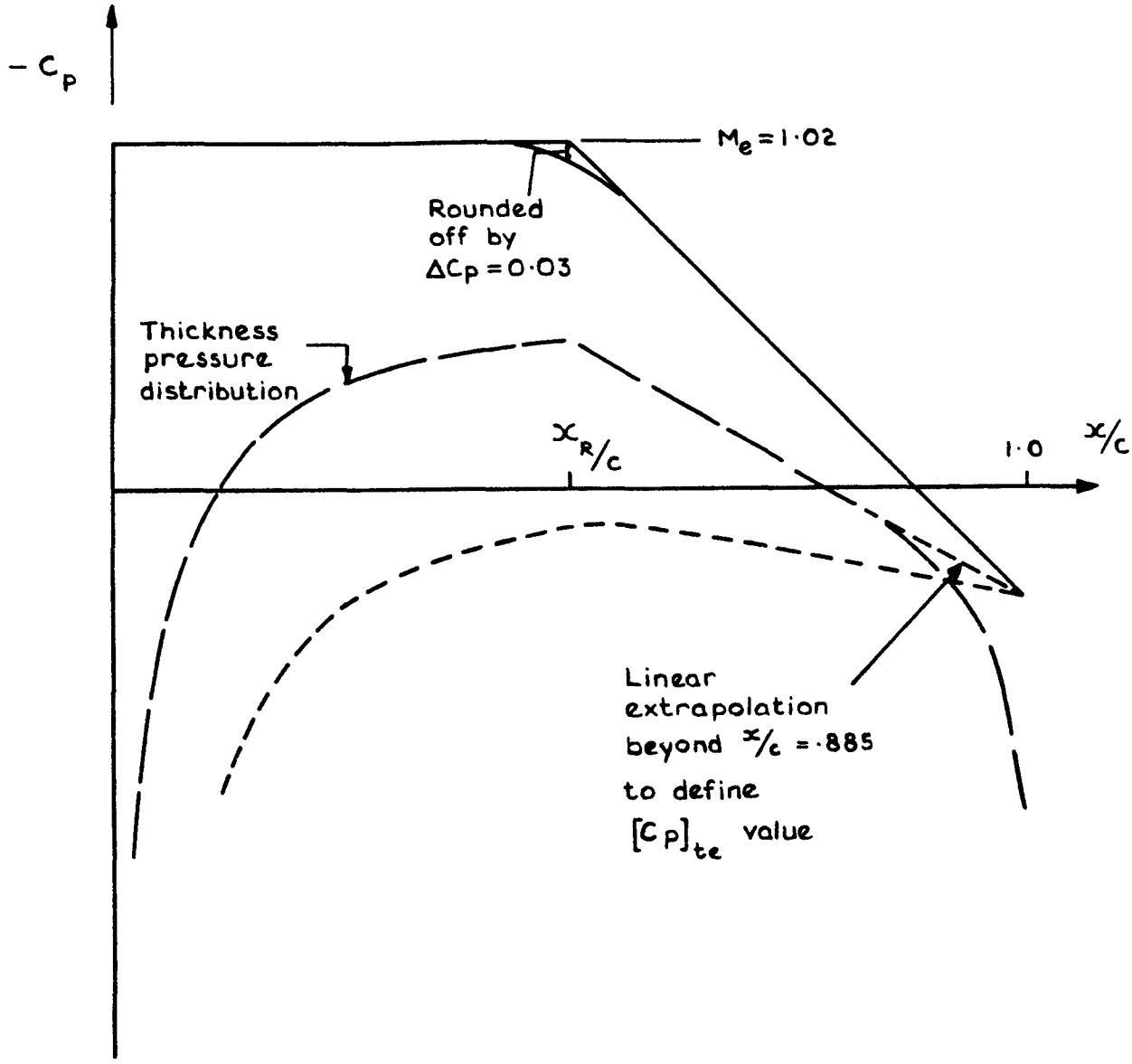

Fig. 1 Sketch defining TDM specification of aerofoil design pressures (See Ref 2)

circulation being found for a forward upper-surface transition and a rearward position on the lower surface.

Figs.13 and 14 show that there is little dependence of the drag of one surface on the conditions on the other so that the existing presentation in Ref.3 can be retained.

3.2 Results of calculations at design C_L, and comparison with the original aerofoil family

3.2.1 The design point (drag-rise) loci

The results for the 50% rooftop aerofoils (extracted from Ref.12) are reproduced here, as Fig.15, and are entirely typical. The loss of lift as compared with the aerofoils of Ref.2 varies from about 1% for the thicker sections at the lower design Mach numbers (e.g. 101-14-30-70, 103-14-50-70 sections) to about 10% for the thinner more highly cambered sections with the largest values of $C_{L_{des}}$ (e.g. 104-06-60-70, 103-06-50-70). The design lift coefficients are compared, in Table 1, with the original values from Ref.2. The new values for the 102 series, which have 40% rooftops, are close to those found by Hodges[9] and confirm that the estimates in TDM 67009 [2] were overoptimistic resulting from the less accurate compressibility corrections used originally.

3.2.2 The design pressure distributions and camber lines

Ref.12 gives the pressure distributions and section ordinates for the complete family of new aerofoils designed at the 'mean' design condition of $R_c = 10^7$ and $x_{tr}/c = 0.05$. Comparisons are made here only for the 50% rooftop sections.

Fig.16 shows the effect on the inviscid designs of changing the compressibility law from the original Wilby expression as used in Ref.2, to that devised by Lock[8]. The new compressibility law produces a loss of lift and of camber; the effect becomes more significant as t/c falls. Fig.17 then shows the effect of including viscous effects in the design process; the new compressibility law being used in each case for the calculation of pressures. The introduction of viscous displacement effects raises the camber progressively as t/c rises and the influence of the displacement thickness at the trailing edge gives rise to a lowered pressure there. Consequently, the combined effect (see Fig.18) is to reduce loading and camber over the forward part of the section but to increase these over the rear, by an amount that rises with t/c.

3.2.3 Profile drag

Cosby shows, in Ref.12, a series of graphs in which the new values of C_{D_u}, C_{D_ℓ} and C_D are plotted against the corresponding original values[13]. One such graph is reproduced here as Fig.19, for the 50% rooftop sections. This figure shows that the new total drag coefficients exhibit a constant increment over the old values which seems to be independent of Reynolds number, transition position or t/c. This is found to be true, for C_{D_u}, C_{D_ℓ} and C_D at a given x_R/c and M_{des}, over the whole range of conditions covered by the new family. Consequently, the complete set of carpet plots for profile drag need not be replaced by new ones; only the differences need be plotted as in Fig.20. That is, as

$$C_{D_u}, C_{D_\ell}, C_D = f(M_{des}, x_R/c) \quad .$$

For completeness, the new carpets of profile drag are plotted out in Ref.12 and compared with the originals. As an example, the carpets for 103-14-50-70 are shown here as Fig.21.

3.2.4 Lift/drag ratio

The loss of performance of the new sections when compared with the original family is clearly demonstrated by Fig.22. Again, attention is restricted here to the 50% rooftop sections but the other sections show similar behaviour.

3.2.5 Trailing edge pressures and rear separation

The trailing edge pressures, estimated from the extrapolation of inviscid pressures of the original family, were unrealistically large, except for very large Reynolds numbers, as Fig.23 shows. The strong variation of $[C_p]_{te}$ with transition position and Reynolds number also results in considerable differences between the new rear separation boundaries predicted by Stratford's method and those obtained earlier. Fig.24 shows this for the 103 series aerofoils. The gain in operating Reynolds number for attached flow over the original estimates becomes larger as the sections become thicker. This is due to the greater relaxation of adverse pressure gradients on the upper surface (see Fig.12, for example).

4 CONCLUSIONS

The comparisons of the new pressure and lift values with those of the original family show that:

(i) The new sections have design lift coefficients lower by 0 to 10%, at given M_{des}, t/c, x_R/c. They generally have slightly increased rear loading and camber, because viscous displacement effects are now included in the design, but reduced forward loading due to the changed compressibility law.

(ii) The new trailing edge pressures depend strongly upon transition position and R_c and show that the original estimated values were unrealistically high.

(iii) Consequently, the new sections have a much larger range of attached flow conditions than the original calculations indicated.

The profile drag comparisons show that:

(iv) The new sections have, for a given M_{des} and x_R/c, a constant increment in profile drag over the earlier aerofoils irrespective of Reynolds number, t/c or transition position.

Hence,

(v) The performance (e.g. in terms of C_L/C_D) associated with the original family is too high and the new sections are thought to be much more realistic.

(iv) The present method of aerofoil design is supported by comparison with the newer method due to Firmin. Despite the crude nature of the present drag prediction procedure, it seems to be as reliable as present experimental results although neither transitional nor three-dimensional phenomena are accounted for properly in existing comparisons between theory and experiment.

Finally,

(viii) Some experimental work is clearly needed to establish criteria for significant separation effects, even in the absence of shocks.

Acknowledgments

The authors are grateful for encouragement from Dr. R.C. Lock, and for valuable suggestions regarding presentation from Mr. M.D. Hodges of the Royal Aeronautical Society, Engineering Sciences Data Unit.

Table 1

COMPARISON OF DESIGN LIFT COEFFICIENTS OF THE NEW SECTIONS WITH THE ORIGINAL TDM VALUES

Section	New $C_{L_{des}}$	Original $C_{L_{des}}$
101-10-30-65	0.823	0.87
101-14-30-65	0.657	0.66
101-06-30-70	0.69	0.75
101-10-30-70	0.505	0.53
101-14-30-70	0.312	0.30
101-06-30-75	0.438	0.48
101-10-30-75	0.222	0.23
101-06-30-80	0.208	0.22
102-10-40-65	0.924	0.98
102-14-40-65	0.769	0.79
102-06-40-70	0.767	0.84
102-10-40-70	0.587	0.63
102-14-40-70	0.403	0.40
102-06-40-75	0.496	0.55
102-10-40-75	0.289	0.30
102-06-40-80	0.255	0.28
103-06-50-70	0.849	0.93
103-10-50-70	0.673	0.72
103-14-50-70	0.496	0.50
103-06-50-75	0.557	0.62
103-10-50-75	0.36	0.38
103-06-50-80	0.304	0.33
104-06-60-70	0.919	1.01
104-10-60-70	0.751	0.81
104-14-60-70	0.581	0.59
104-06-60-75	0.618	0.69
104-10-60-75	0.425	0.44
104-06-60-80	0.340	0.38

NOTATION

c	chord length
c_f	local skin-friction coefficient $(= \tau_0/\frac{1}{2}\rho_e u_e^2)$
G	boundary-layer similarity parameter $\left(= \frac{1}{u_\tau} \int_0^\infty (u_e - u)^2 dy \Big/ \int_0^\infty (u_e - u) dy \right)$
H	boundary-layer shape factor $= \delta^*/\theta$
s	arc length around aerofoil surface in chordwise plane, measured from leading edge stagnation point
t	aerofoil thickness
u	velocity component within boundary layer
u_e	free stream velocity locally
x	distance along chord
α	angle of incidence
δ^*	boundary-layer displacement thickness
θ	boundary-layer momentum thickness
π	$\left(= \frac{\delta^*}{\tau_0} \frac{dp}{dx} \right)$ equilibrium pressure gradient
τ_0	local surface shear stress

Subscripts

des	design point value $\left(\text{e.g. } C_{L_{des}}, C_{D_{des}} \right)$
D	drag-rise value, in this context also the design point value $\left(\text{e.g. } C_{L_D}, M_D \right)$
R	end of rooftop value (e.g. x_R/c)
tr	transition point value (e.g. x_{tr}/c)
u	upper surface
ℓ	lower surface
te	trailing edge (e.g. $[C_p]_{te}$)
e	local free stream value (e.g. M_e)

NOTATION (concluded)

TDM section designation:

(Member of RAE 100 series thickness forms) - (% t/c) - (100 × rooftop length x_R/c) - (100 × design Mach number M_D): e.g. 103-14-50-70 has a 14% thick RAE 103 thickness distribution, constant upper-surface pressure (M_e = 1.02) up to x/c = 0.50, and a design (drag-rise) M = 0.70.

REFERENCES

No.	Author	Title, etc.
1	I.H. Abbott A.E. von Doenhoff	Theory of wing sections. McGraw-Hill, New York (1949)
2		Transonic Data Memorandum. Drag-rise Mach number of aerofoils having a specified form of upper surface pressure distribution: Charts and comments on design. Eng. Sci. Data Item No. 67009 (1967)
3		Transonic Data Memorandum. Aerofoils having a specified form of upper surface pressure distribution: Details and comments on design. Eng. Sci. Data Item No. 67010 (1967)
4		Method for predicting the pressure distribution on swept wings with subsonic attached flow. Roy. Aero. Soc. Transonic Data Memorandum 6312 (1963)
5	P.G. Wilby	The calculation of subcritical pressure distributions on symmetric aerofoils at zero incidence. ARC CP No.993 (1967)
6	J.F. Nash A.G.J. Macdonald	The calculation of momentum thickness in a turbulent boundary layer at Mach numbers up to unity. ARC CP No.0963 (1966)
7	C.C.L. Sells	Plane subcritical flow past a lifting aerofoil. RAE Technical Report 67146 (ARC 29850) (1967) Proc. Roy. Soc., A308, pp.377-401 (1968)
8	R.C. Lock P.G. Wilby B.J. Powell	The prediction of aerofoil pressure distributions for subcritical viscous flows. Aero Quart., Vol.21, Part 3 (1970)
9	M.D. Hodges	Calculated values of lift and drag coefficient for certain aerofoils specified as in TDM 67009 but derived using a revised treatment of compressibility effects. ESDU, T.189A (1968)

REFERENCES (continued)

No.	Author	Title, etc.
10	B.J. Powell	The calculation of the pressure distribution of a thick cambered aerofoil at subsonic speeds including the effect of the boundary layer. ARC CP No.1005 (1967)
11	B.J. Powell	Some further computer calculations of the pressure distribution of a thick cambered aerofoil at subsonic speeds including the effect of the boundary layer. NPL Aero. Memorandum 44 (1968)
12	S.W. Cosby	Profile drag, at the drag-rise condition, of a new family of aerofoils designed to have the specified form of upper surface pressure distribution at that condition and including the effects of the boundary layer. Short Bros. and Harland Technical Report AD/TR/GEN/118, S & T Memorandum 14/71 (1970)
13		Transonic Data Memorandum. Profile drag at the drag-rise condition of aerofoils having a specified form of upper surface pressure distribution at this condition. Eng. Sci. Data Item No. 67011 (1967)
14	B.G.J. Thompson S.W. Cosby	The characteristics of a family of rooftop aerofoils designed at their drag rise condition in viscous, compressible flow. Part 2: Off-design conditions. RAE Technical Report 72142 (ARC 34467) (1973)
15	J. Weber	The calculation of the pressure distribution on the surface of thick cambered wings and the design of wings with given pressure distribution. ARC R & M 3026 (1955)
16	B. Thwaites	Approximate calculation of the laminar boundary layer. Aero. Quart., Vol.1, pp.245-280 (1949)

REFERENCES (continued)

No.	Author	Title, etc.
17	N. Rott	Compressible laminar boundary layer on a heat-insulated body. Journ. Aero. Sci., pp.67-68 (1953)
18	M.C.P. Firmin	Calculation of pressure distribution, lift and drag on single aerofoils at subcritical speeds, including an allowance for the effects of the boundary layer and wake. RAE paper unpublished.
19	D.A. Spence	The lift coefficient of a thin jet flapped wing. Proc. Roy. Soc., A238, pp.46-68 (1956)
20	J.E. Green	Application of Head's entrainment method to the prediction of turbulent boundary layers and wakes in compressible flow. RAE Technical Report 72079 (ARC 34052) (1972)
21	H.B. Squire A.D. Young	The calculation of the profile drag of aerofoils. ARC R & M 1838 (1937)
22	P.D. Chappell M.D. Hodges	Note on the effect of wake treatment on profile drag predictions using the J.F. Nash boundary layer development. ESDU, A.150 (1967)
23	P.D. Chappell M.D. Hodges	Comparison of the flow separation point of a turbulent boundary layer in a linear pressure rise as predicted by Stratford's criterion and as implied by the method of Nash, *et al.* for computing the boundary layer growth. ESDU, T.170 (1967)
24	P.D. Chappell	A note on some effects on turbulent boundary layer development of the $(R_\theta)_{tr} \geqslant 320$ criterion in the Nash, Osborne and Macdonald program for estimating profile drag (AX306). ESDU, A.111 (1967)

REFERENCES (concluded)

No.	Author	Title, etc.
25	P.D. Chappell	Some effects of the variation of trailing-edge pressure and rear pressure gradient on aerofoil profile drag as estimated by the method of Nash, *et al.* (NPL program AX306). Roy. Aero. Soc., ESDU,A.115 (1967)
26	J. Osborne	A comparison between predicted and measured profile drag for a two-dimensional aerofoil at incompressible speeds over a large range of Reynolds number. NPL Aero. Note 1052 (ARC 28720) (1967)
27	B.G.J. Thompson G.A. Carr-Hill B.J. Powell	A programme of research into viscous aspects of flow on swept wings. NPL Aero. Note 1100 (ARC 32402) (1970)
28	M.C.P. Firmin T.A. Cook	Detailed exploration of the compressible, viscous flow over two-dimensional aerofoils at high Reynolds numbers. Sixth Congress ICAS, Paper 68-09 (1968)

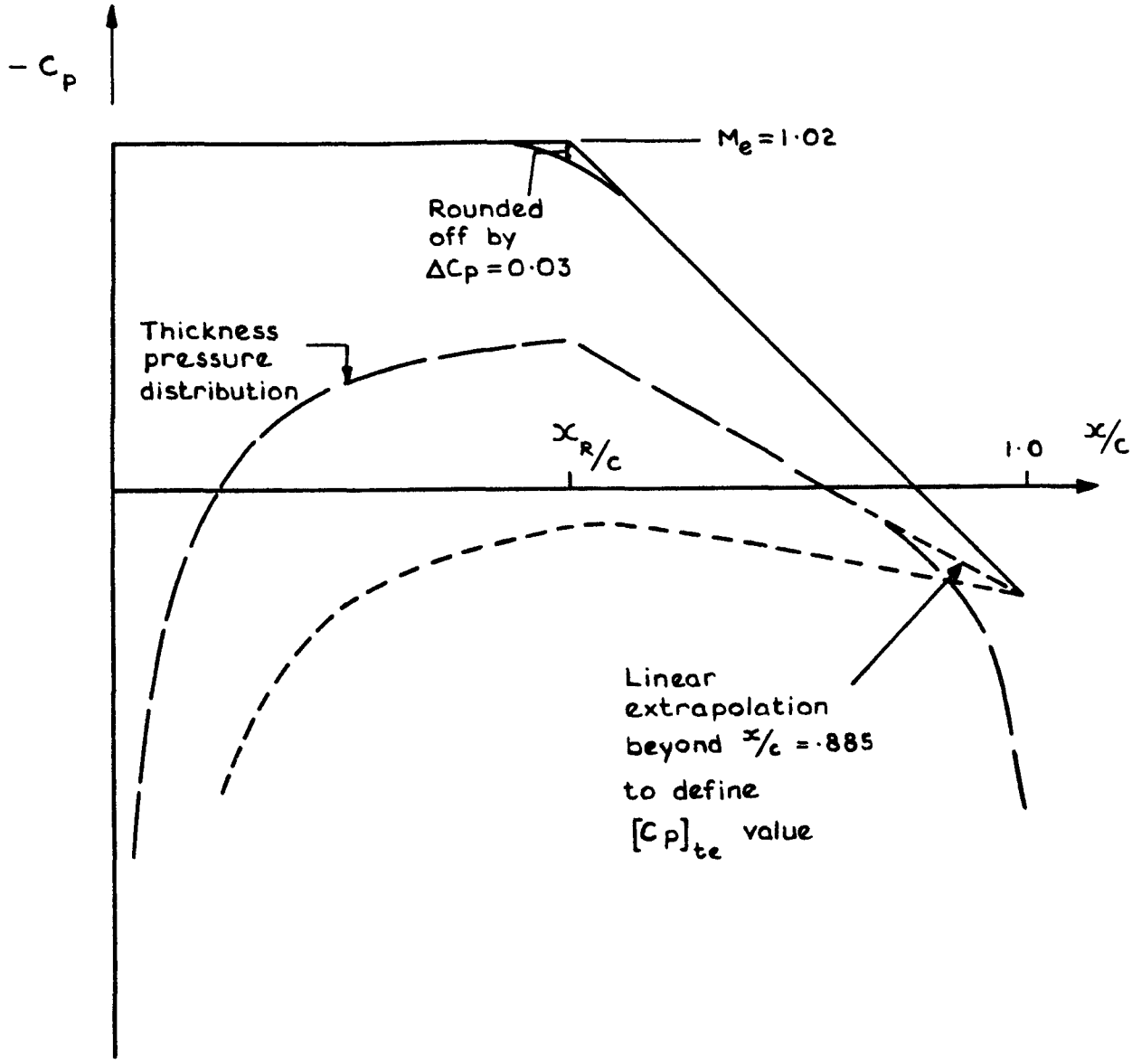

Fig. 1 Sketch defining TDM specification of aerofoil design pressures (See Ref 2)

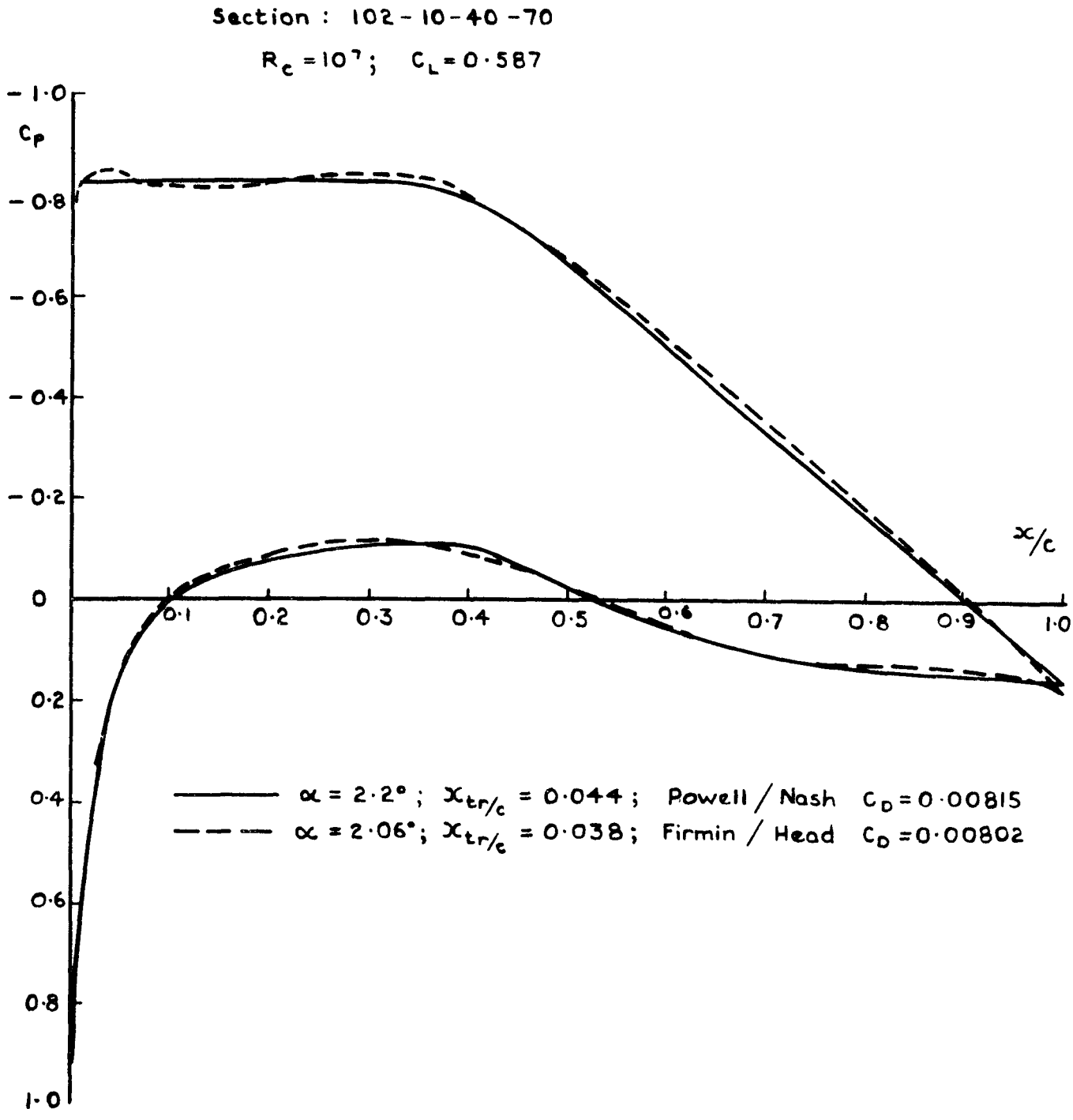

TR 72141

Fig. 2 Comparison of design pressure distribution from the present method with that predicted by Firmin's method (Ref 18) for the same value of lift coefficient

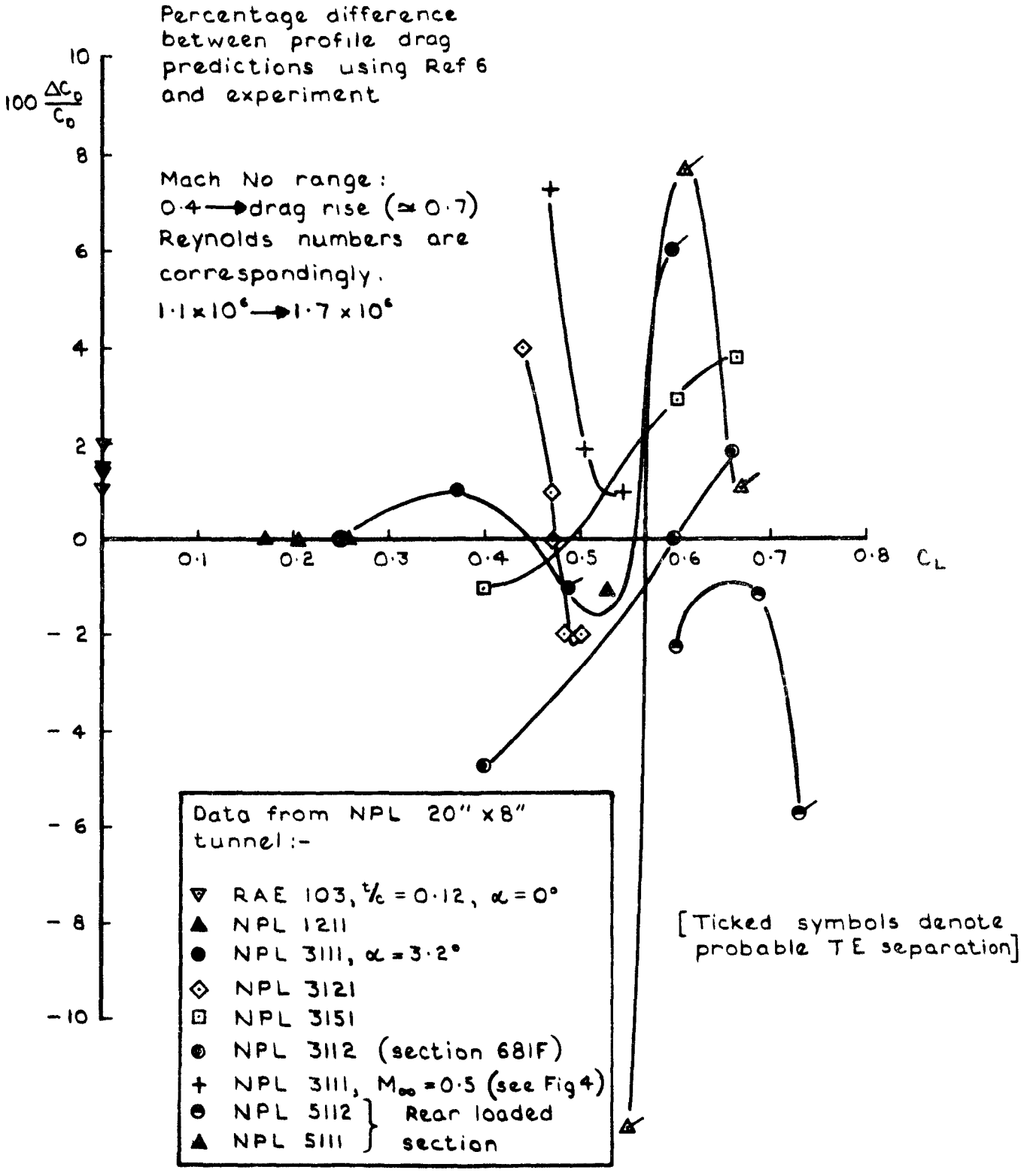

Fig.3 The effect of lift coefficient upon comparisons between drag prediction and experimental results from the RAE (Teddington) 20in x 8in wind tunnel

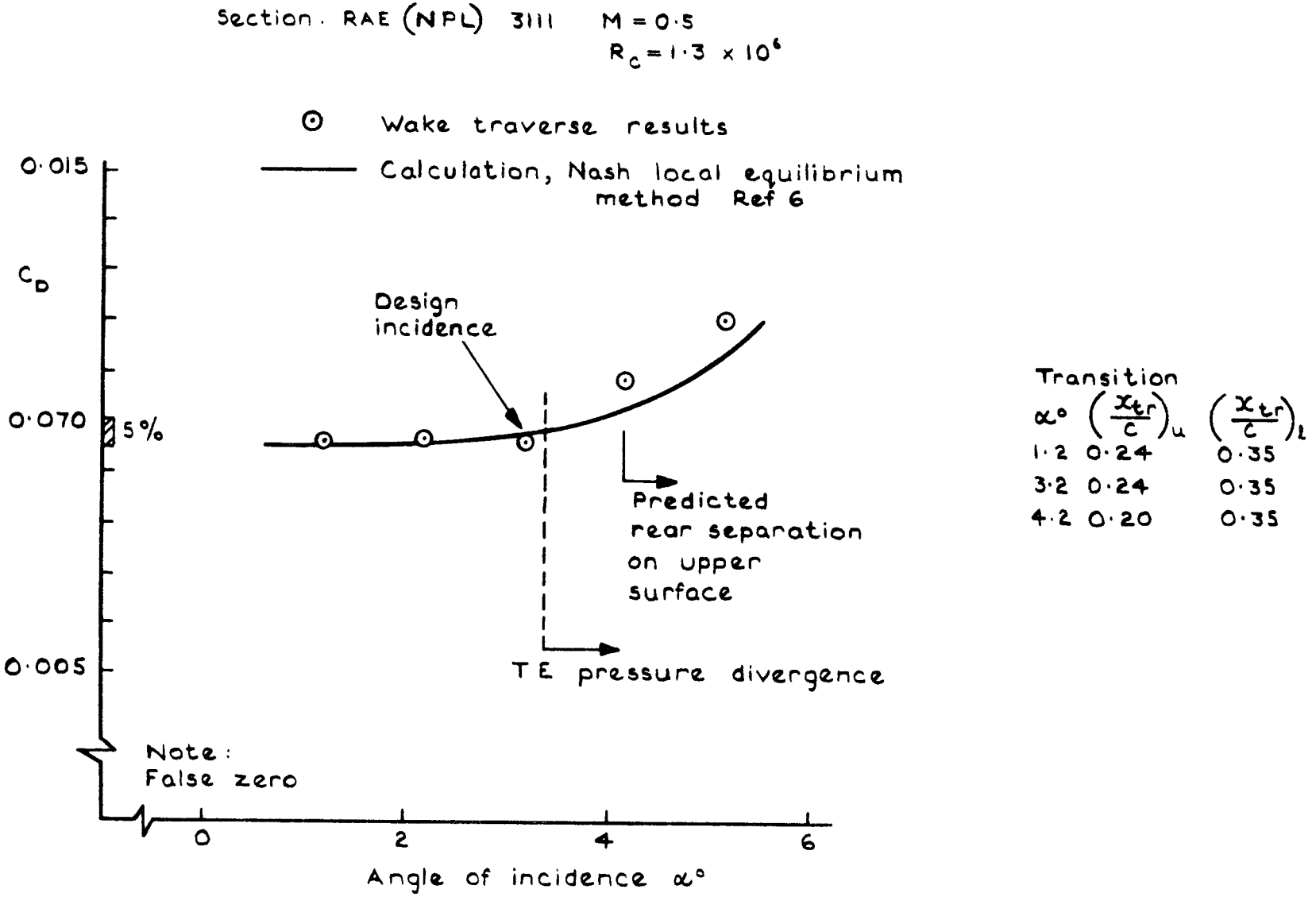

Fig. 4 Comparison of drag prediction and measured values from RAE (Teddington) 20in x 8in wind tunnel

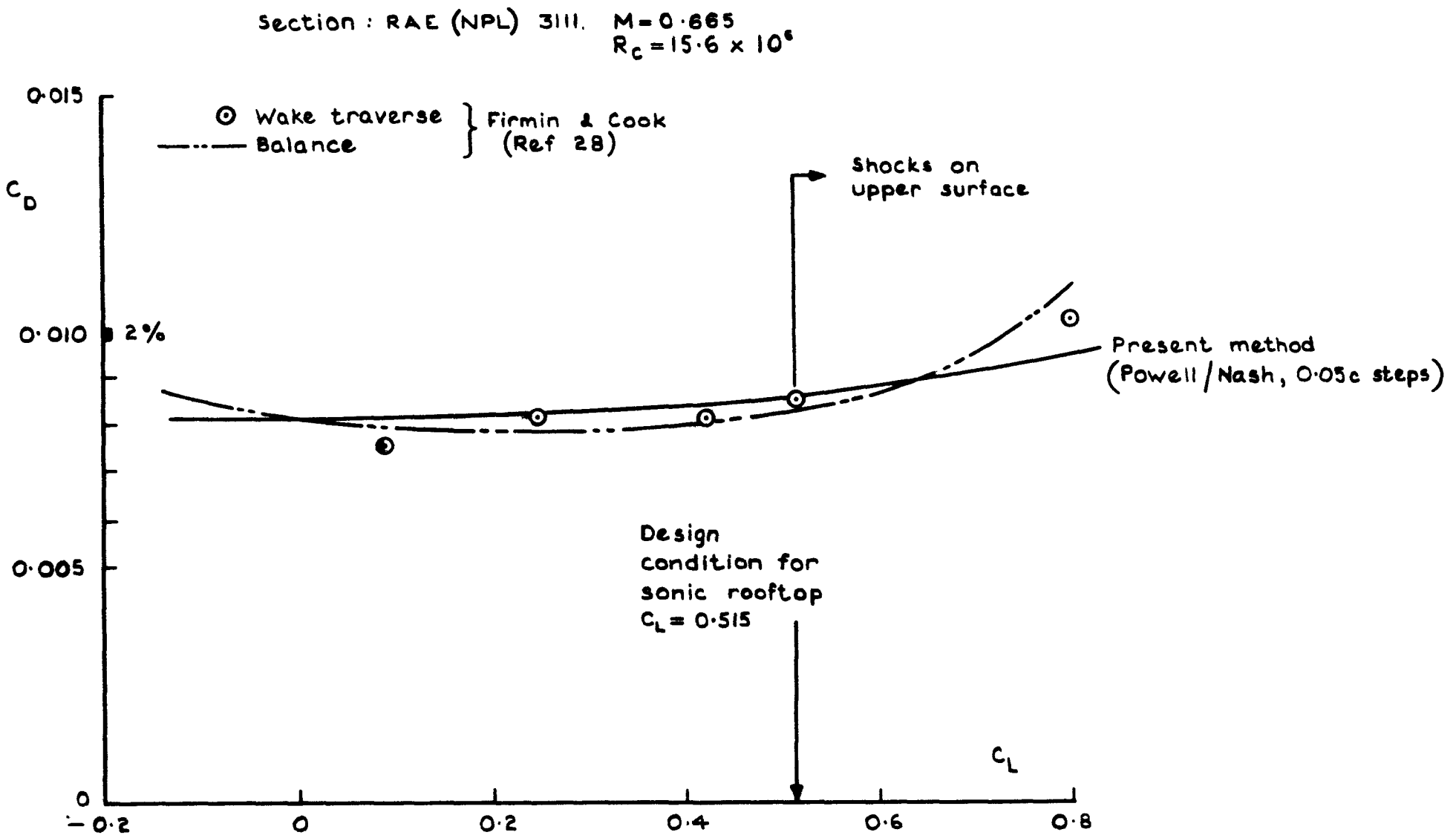

Fig.5 Comparison of drag prediction and measured values from the RAE 8ft wind tunnel

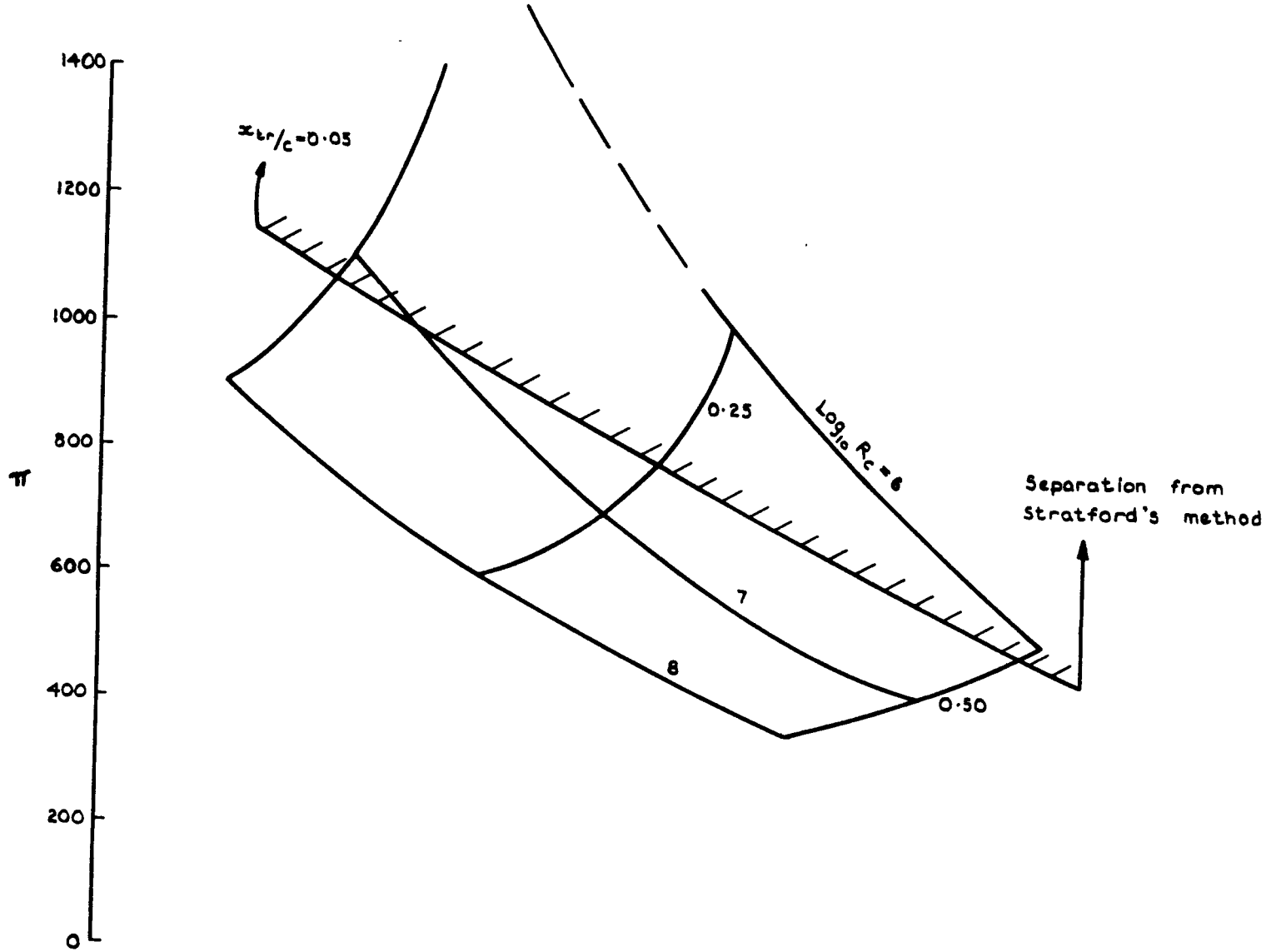

Fig. 6 Variation of π at T.E. over a range of Reynolds number and transition positions, for new 103 – 14 – 50 – 70 aerofoil

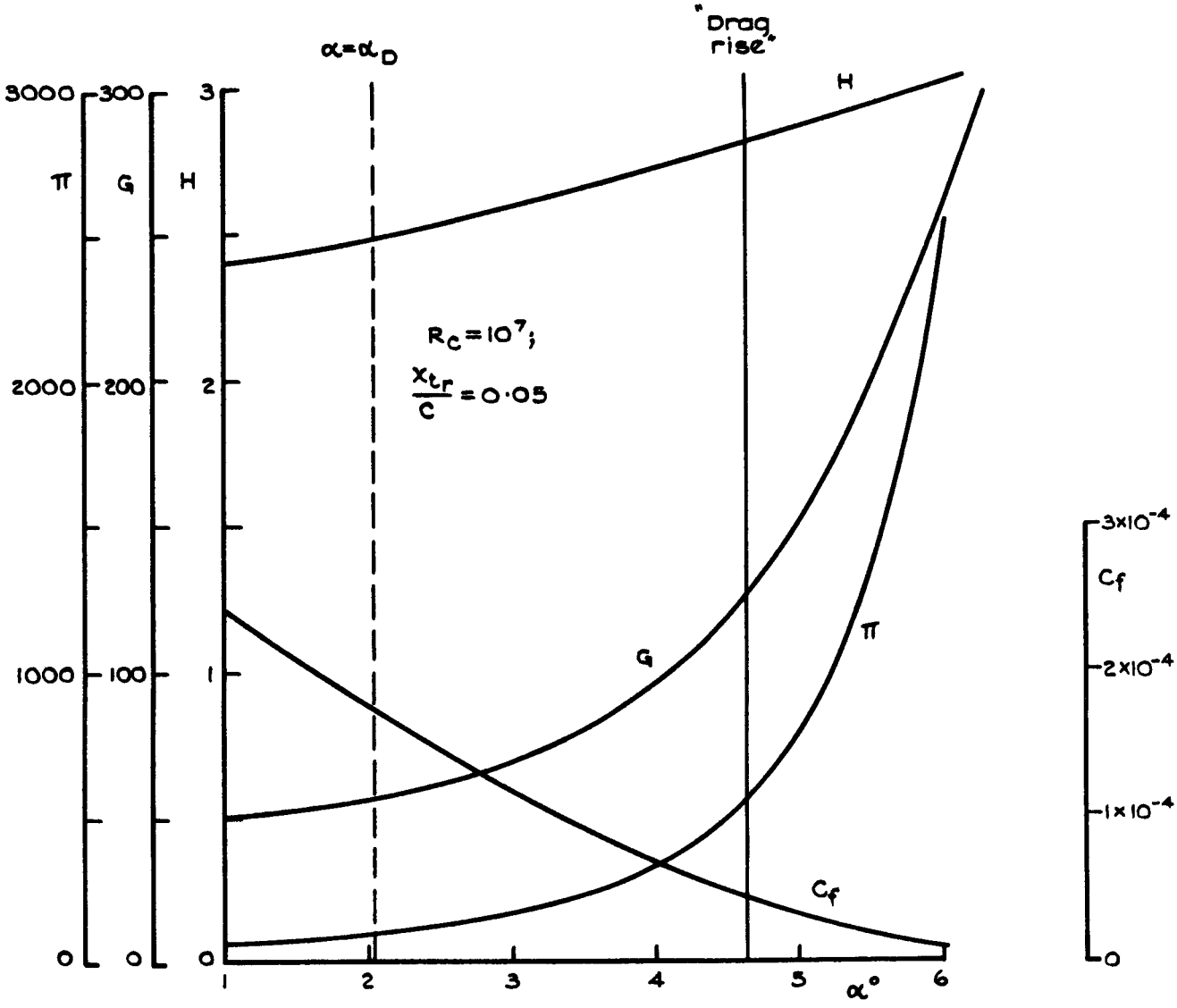

T.R.72141

Fig 7 Variation of trailing edge boundary layer properties with incidence, at M=0·65, for a section designed to have a flat rooftop at M=0·7 (ie section 103-10-50-70)

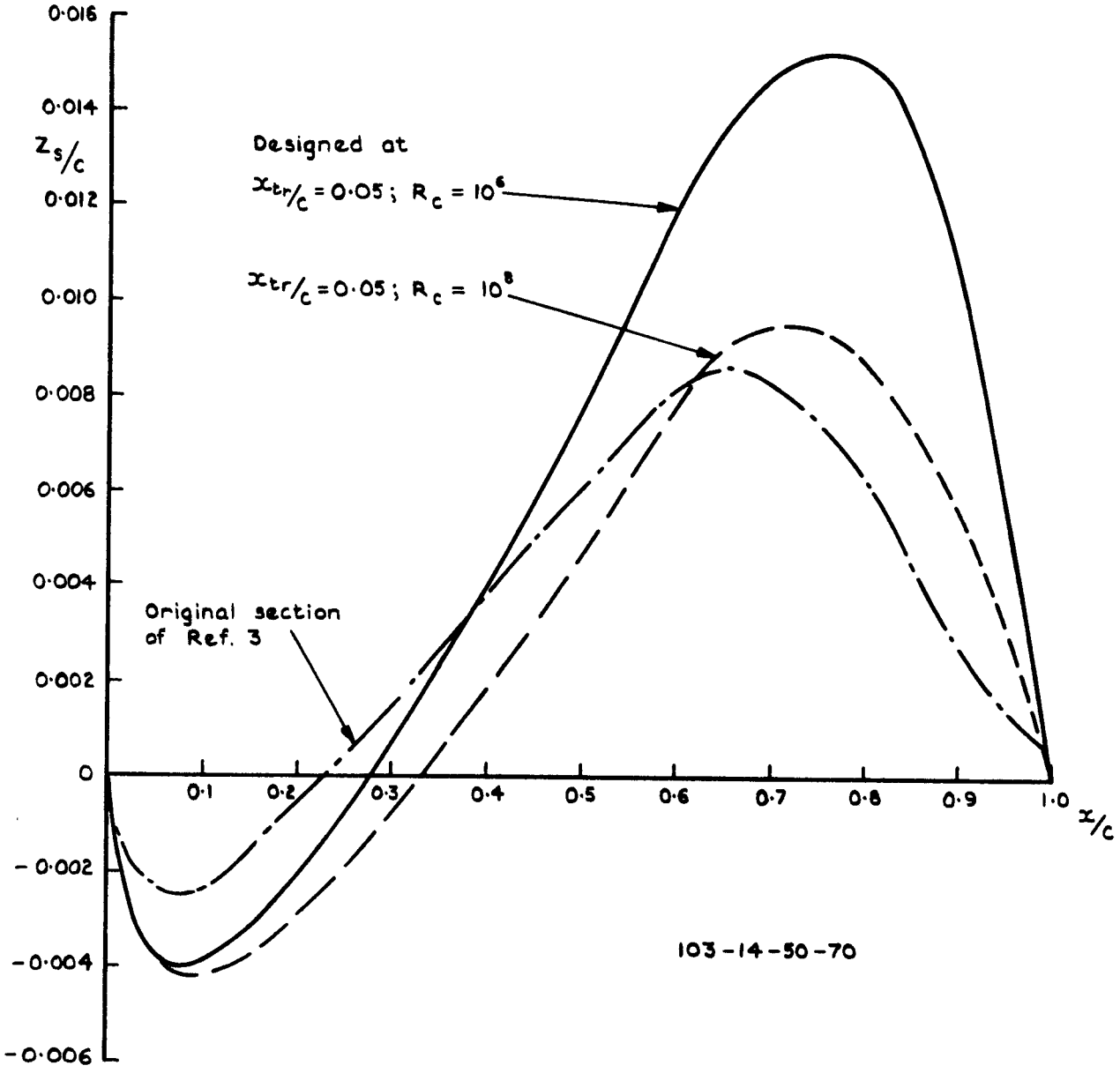

Fig. 8 Effect of Reynolds number on camber lines of inverse designs

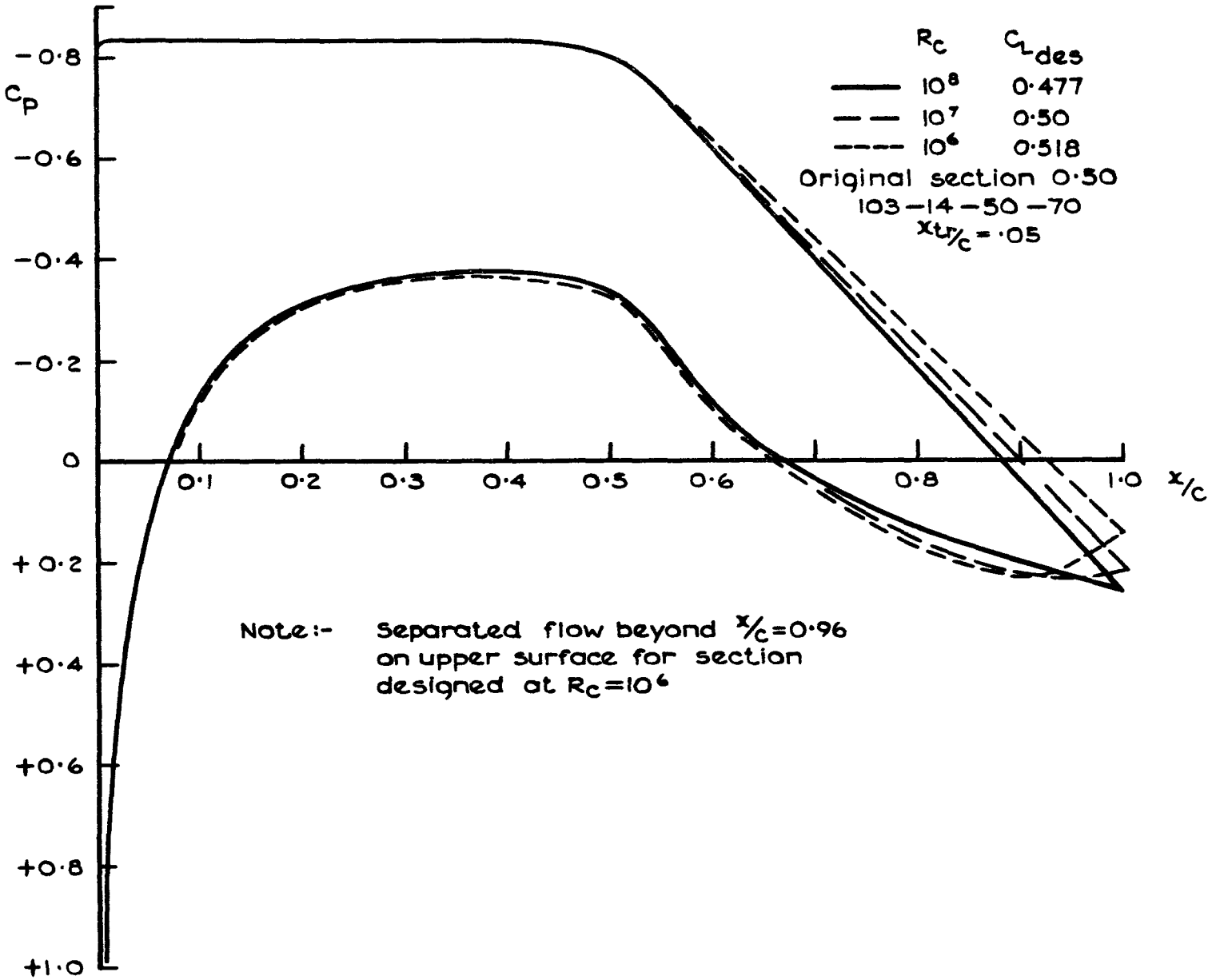

Fig.9 Effect of Reynolds number on inverse designs.
(Having the same transition positions)

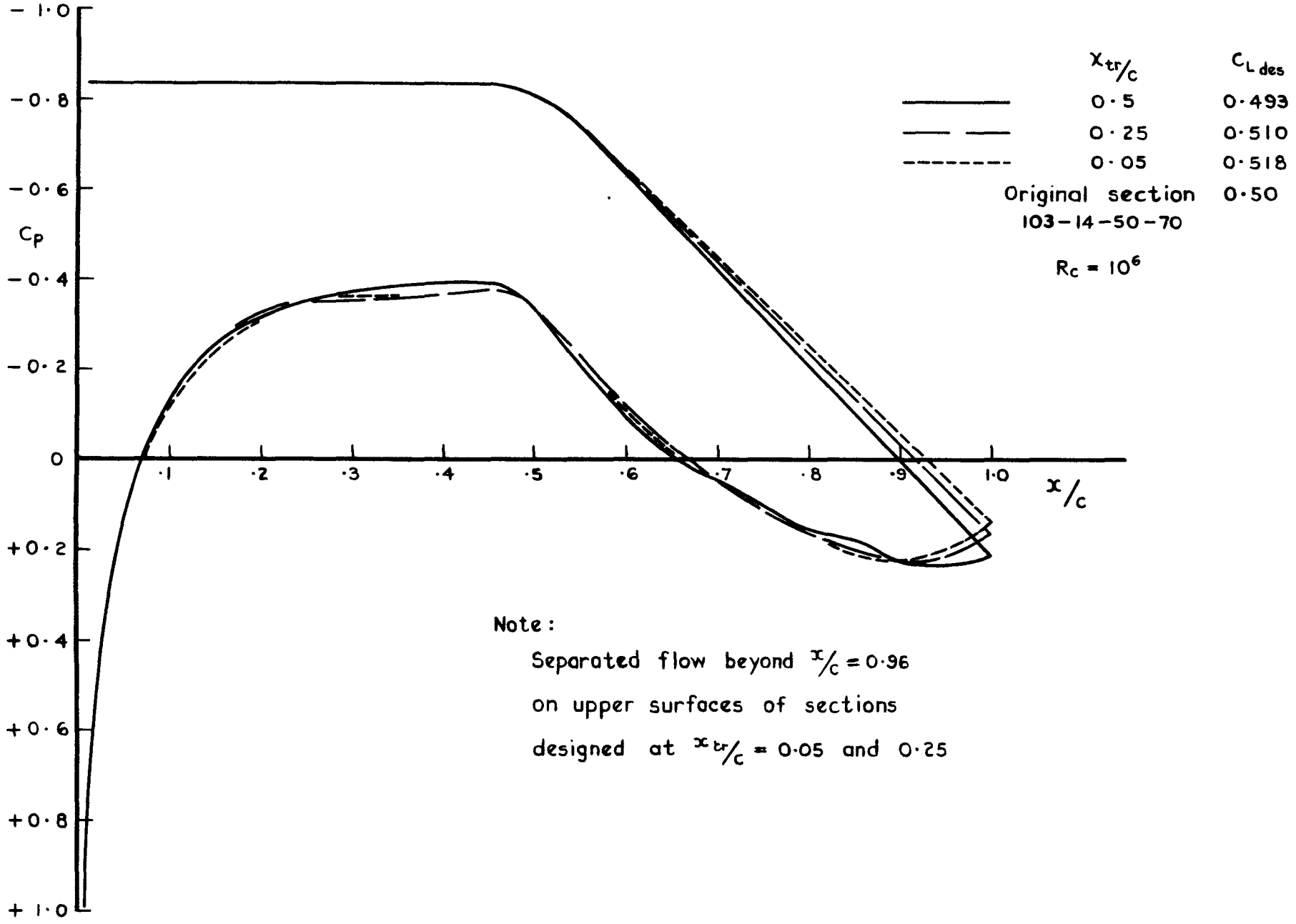

Fig. 10 Effect of transition position on inverse designs (Having the same Reynolds number)

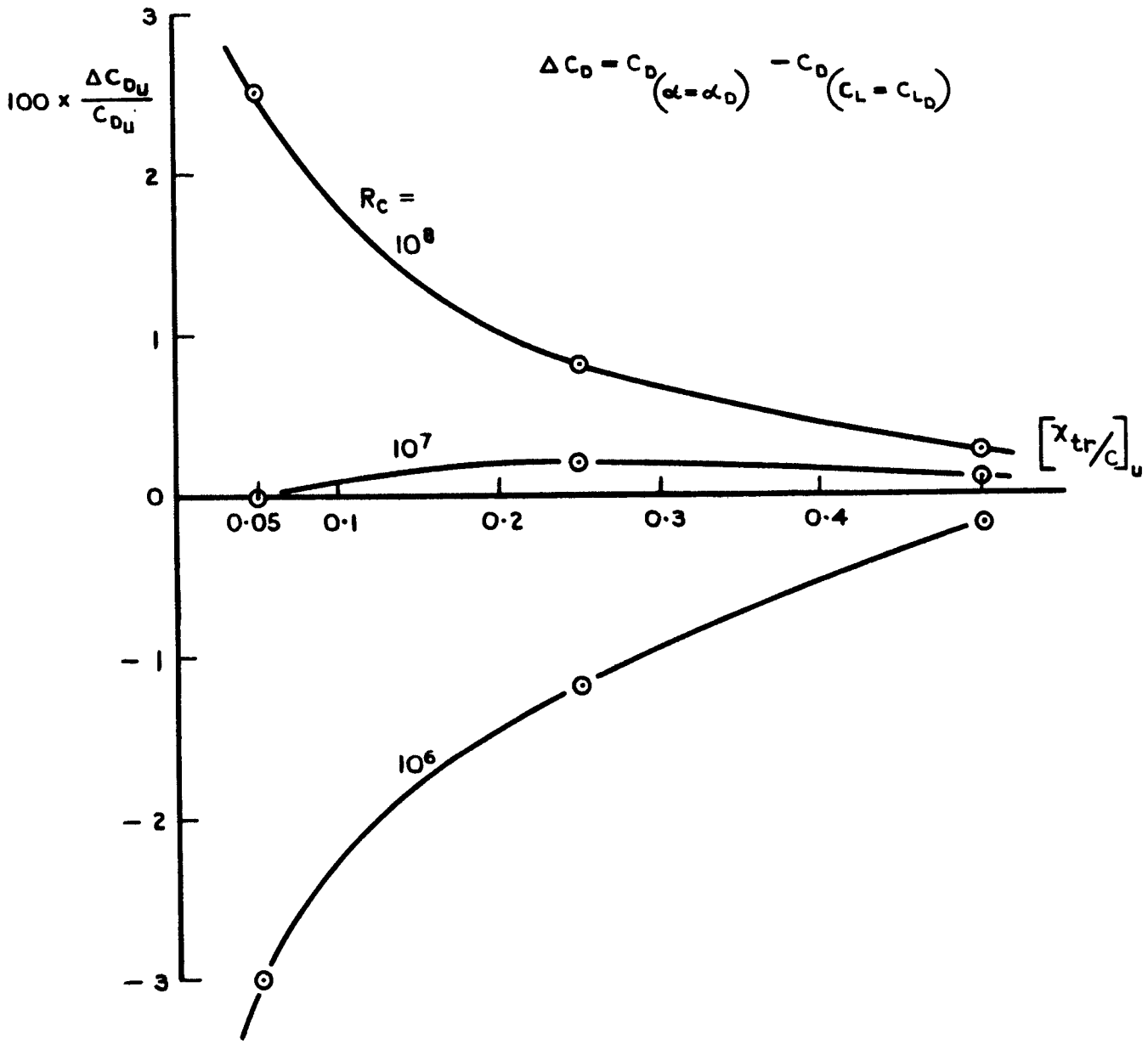

TR 72141

Fig. 11 Effect of incidence correction to give $C_L = C_{L_{des}}$, on upper surface profile drag values
New section: 103-14-50-70 designed at
$R_c = 10^7$, $\left[x_{tr/c}\right]_{u,l} = 0{\cdot}05$

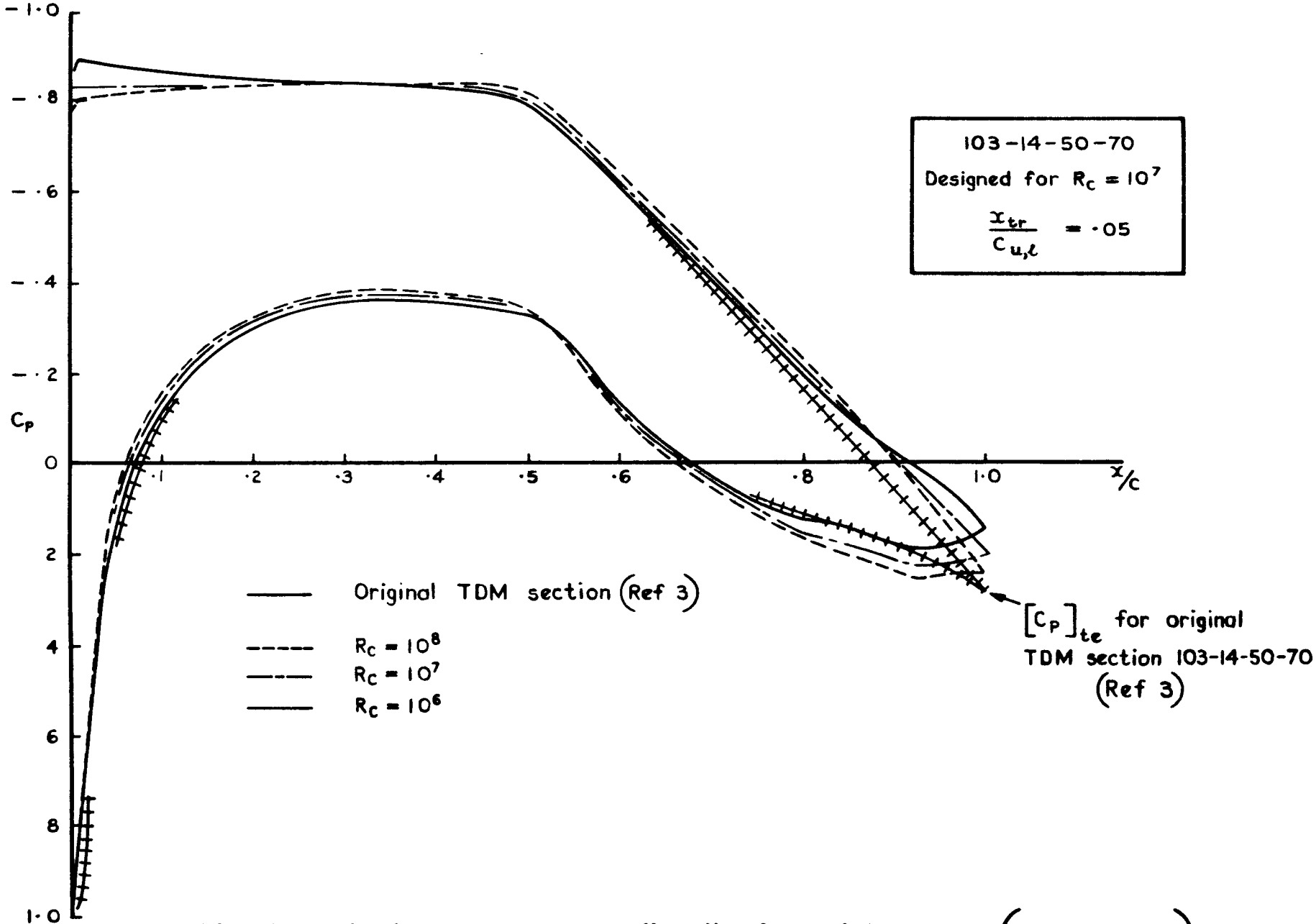

Fig. 12 Variation of pressure distribution with R_c $\left(C_L = C_{L_{des}}\right)$

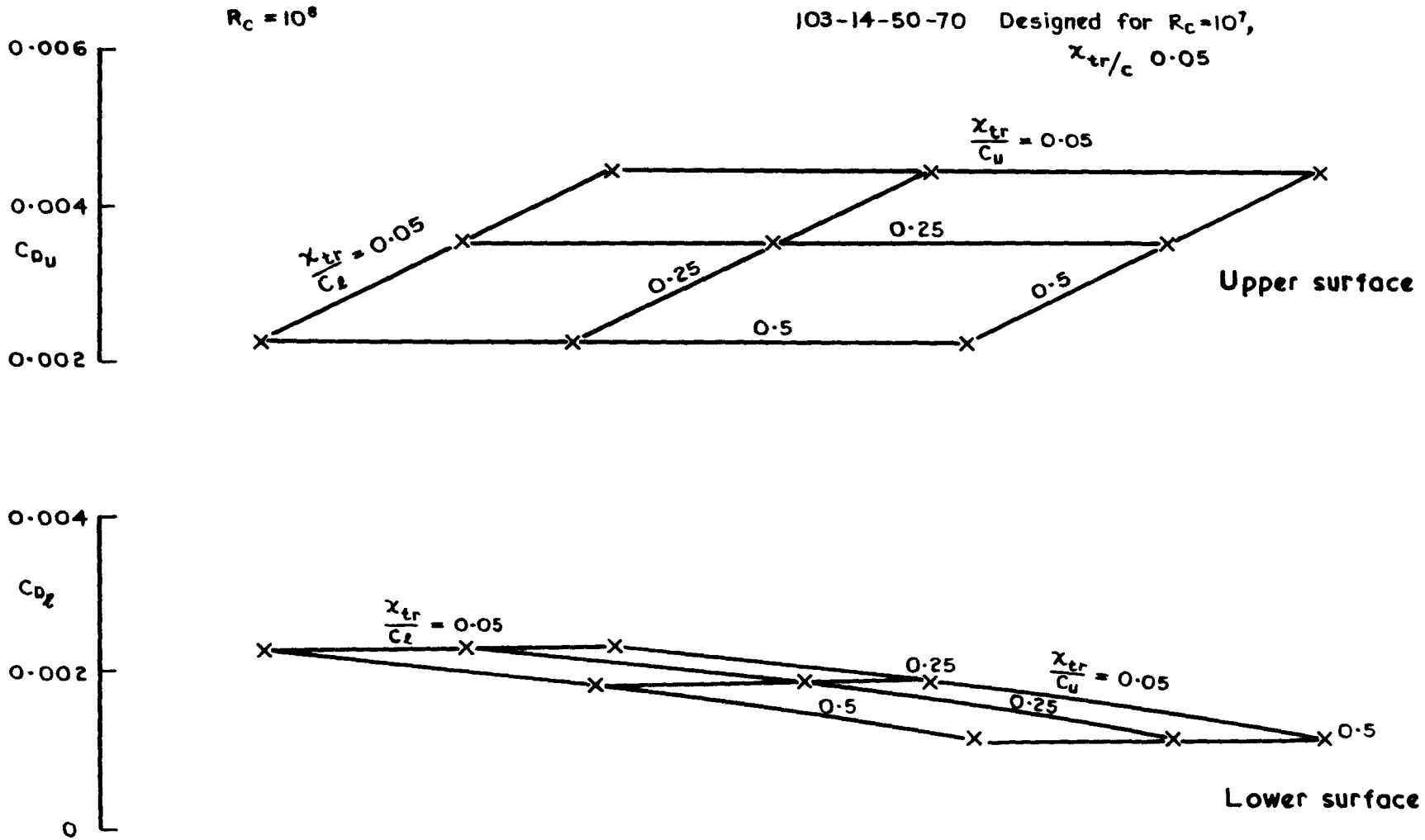

Fig.13 Variation of drag coefficients with upper and lower surface transition positions

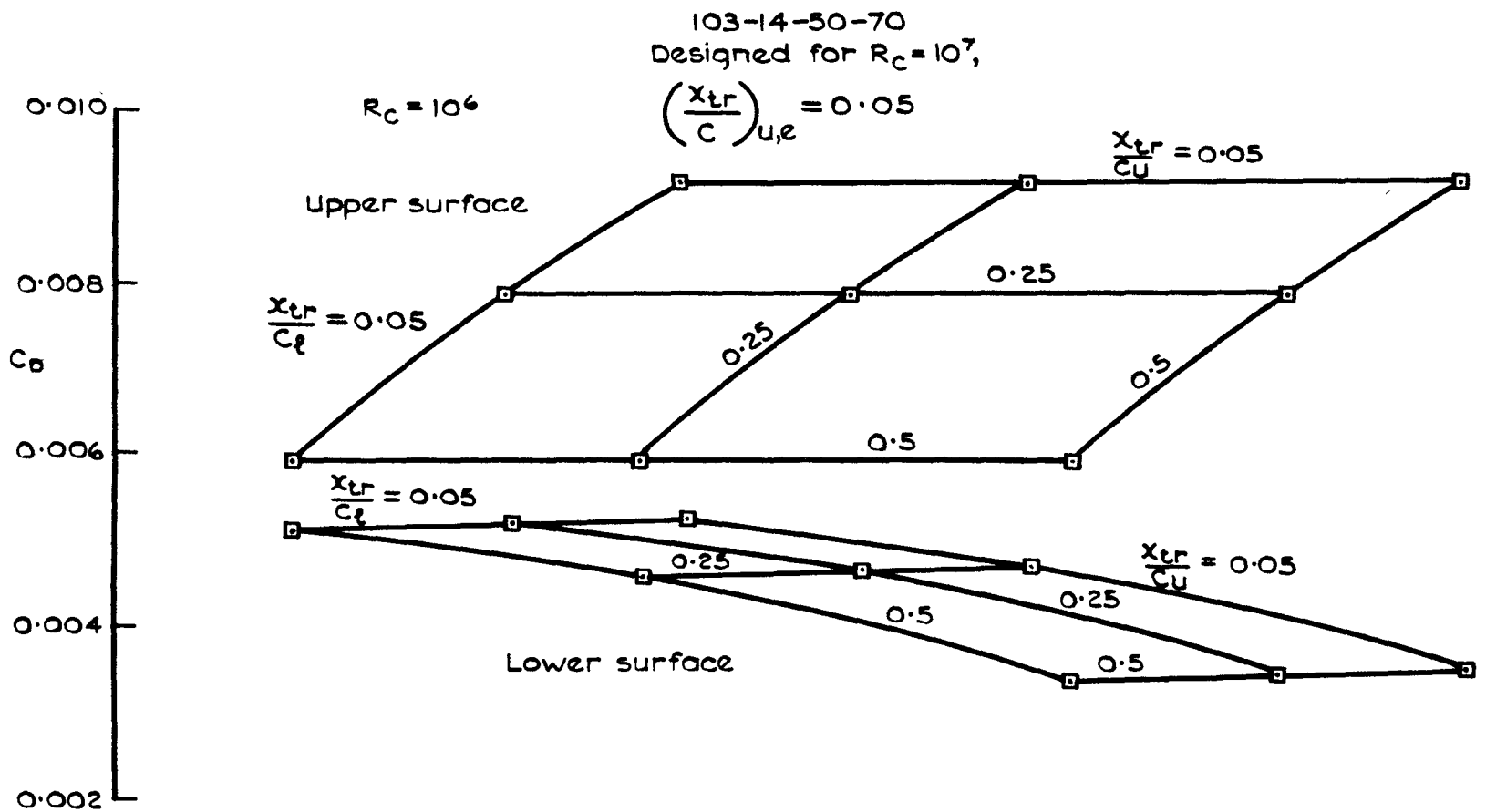

Fig.14 Variation of C_D with upper and lower surface transition positions

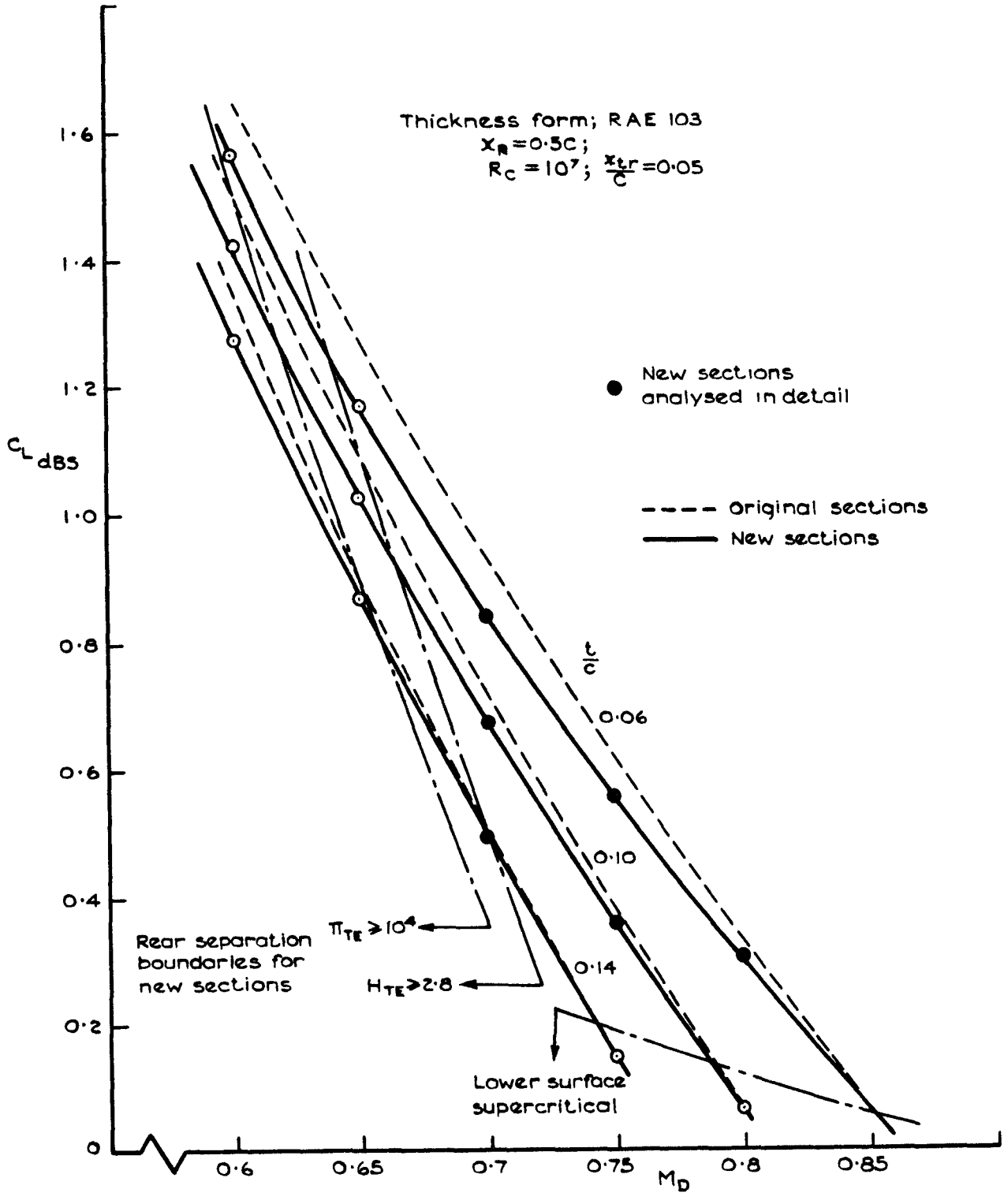

T.R.7214

Fig.15 Comparison of drag-rise loci for original and new aerofoil sections

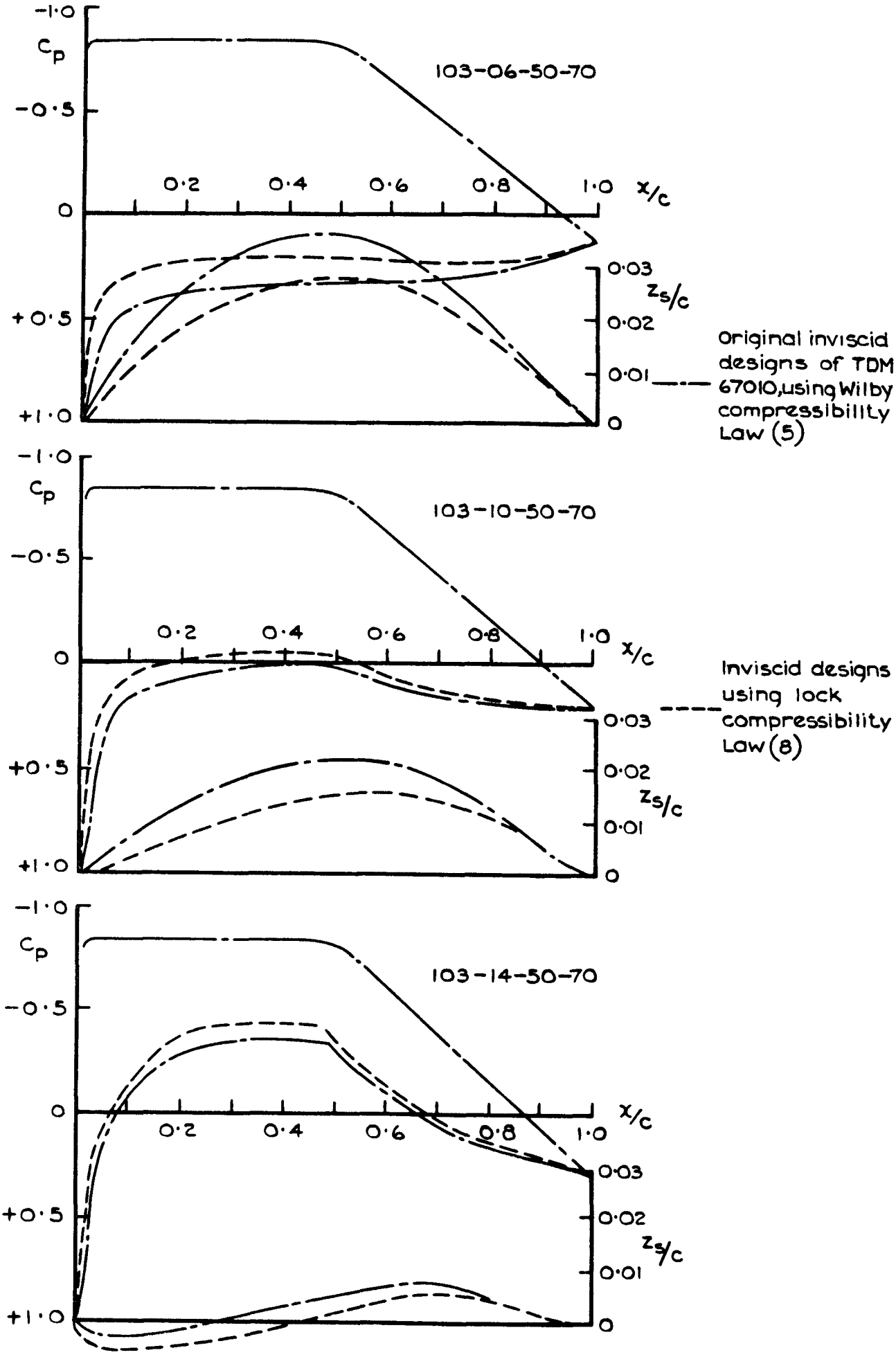

T.R.72141

Fig.16 Effect of using different compressibility laws on pressures and camber lines

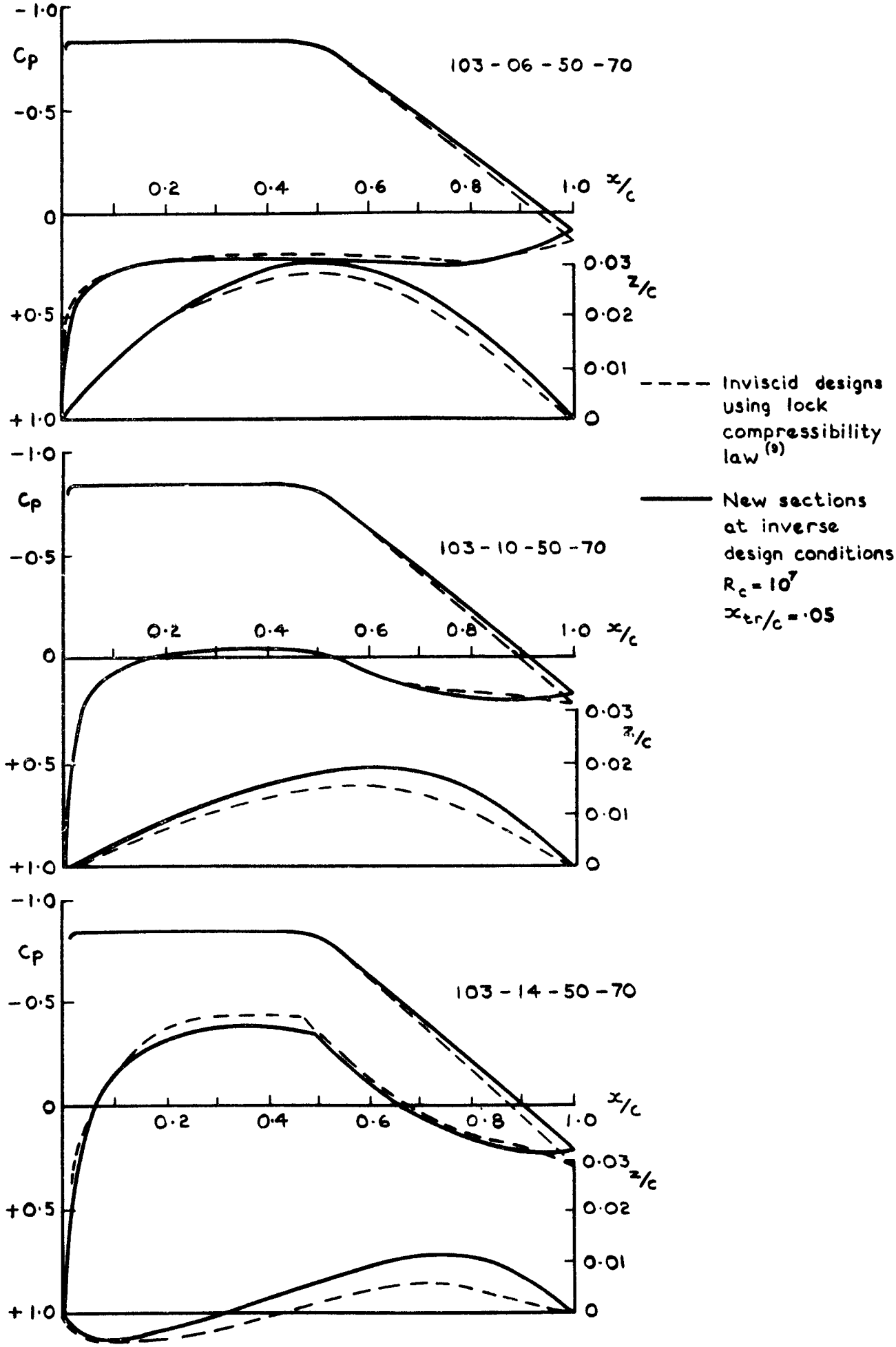

TR 72141

Fig. 17 The effect of viscosity on pressures and camber lines

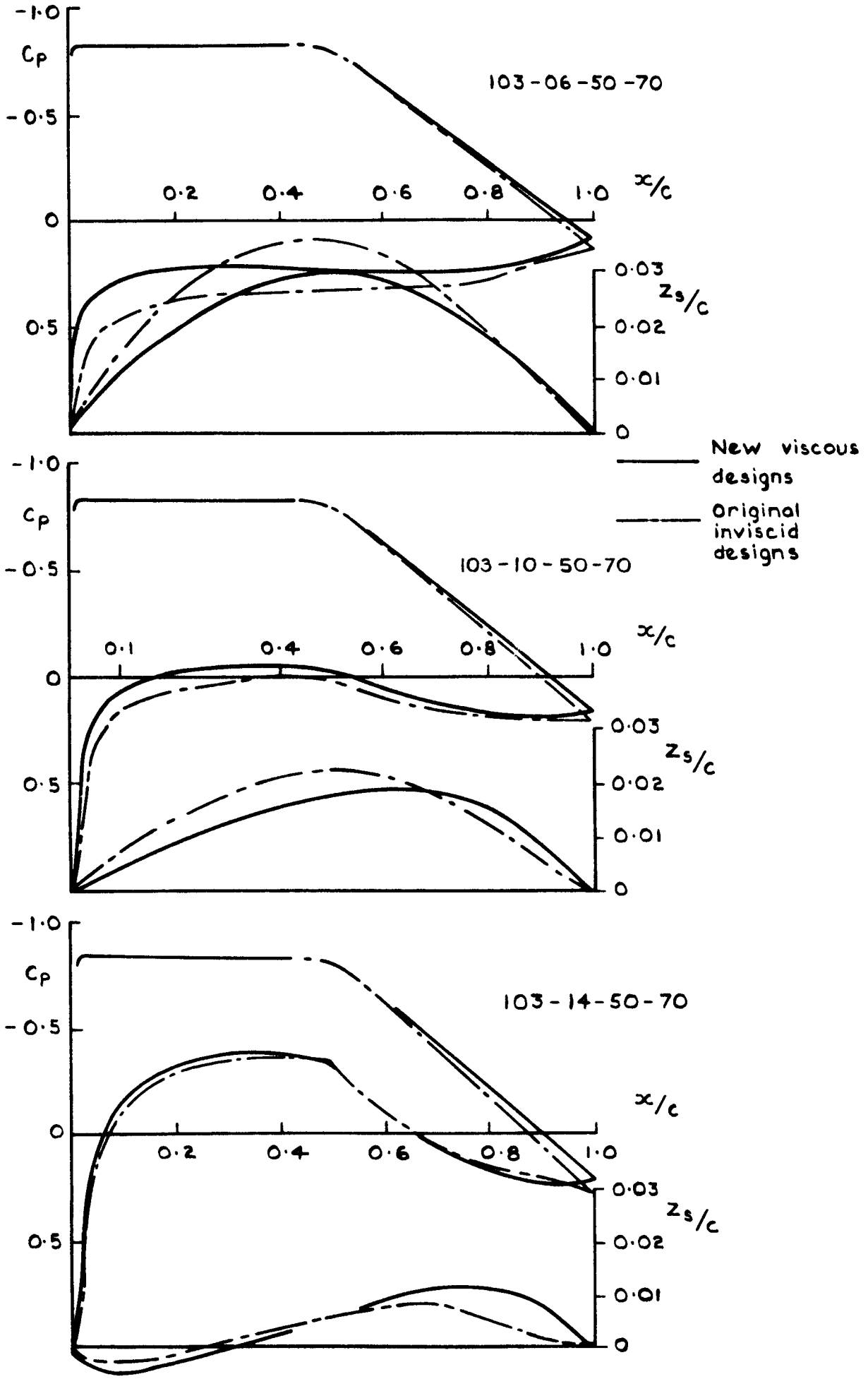

Fig. 18 Comparison of new and original sections (combination of Fig. 16 & 17)

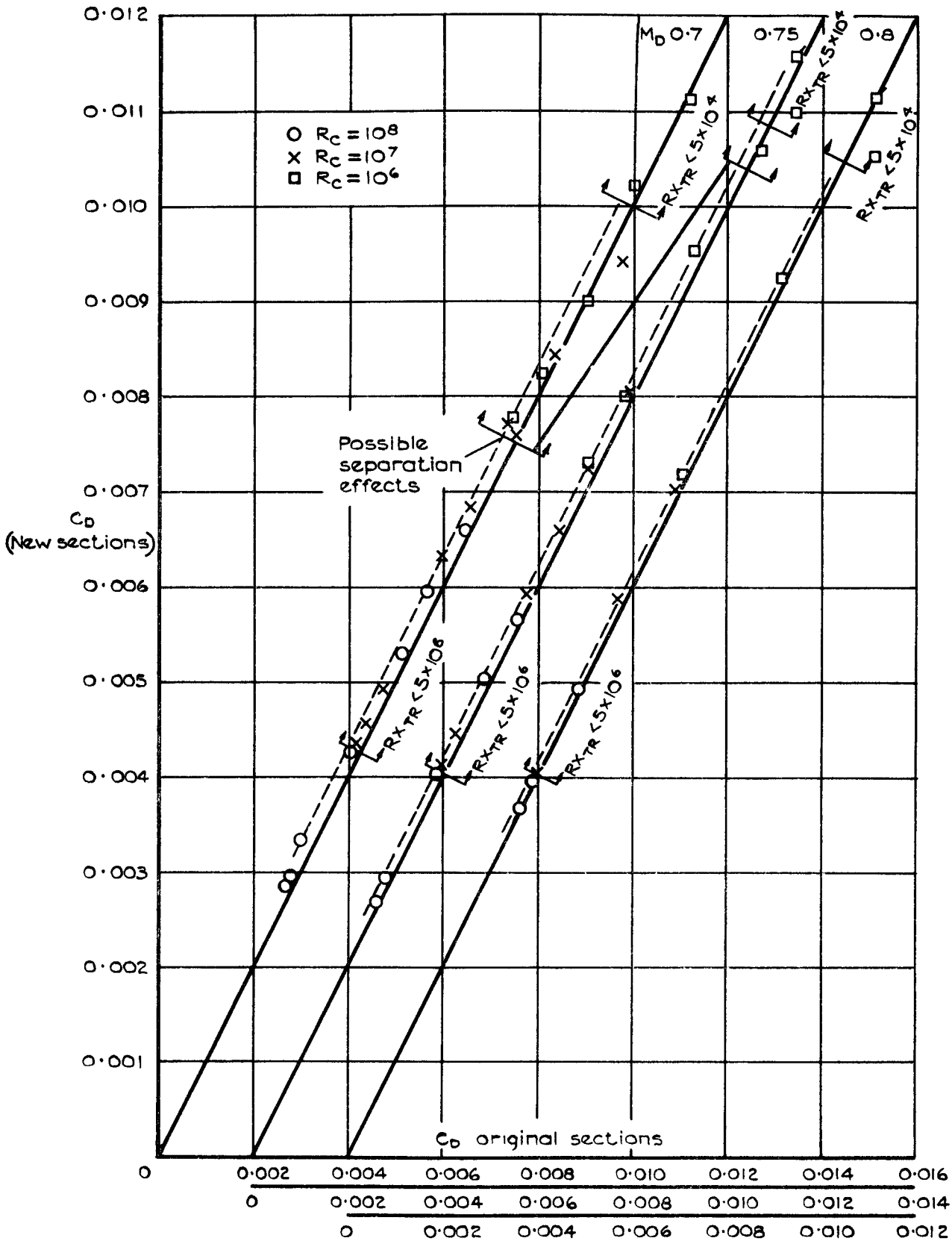

T.R.72141

Fig. 19 Correlation of total drag coefficients for 50% rooftop sections from original family of aerofoils and the new family

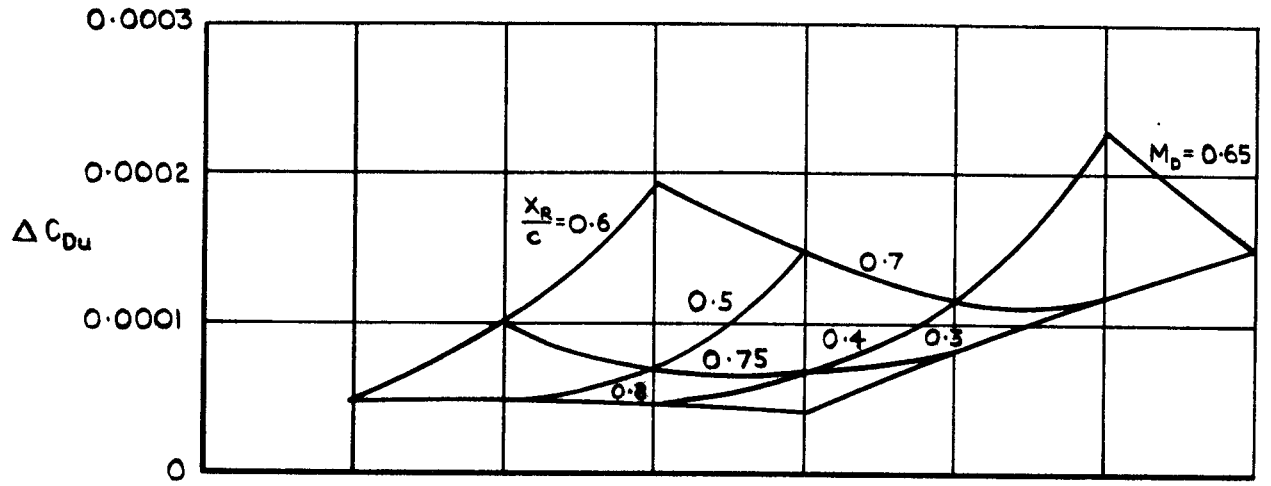

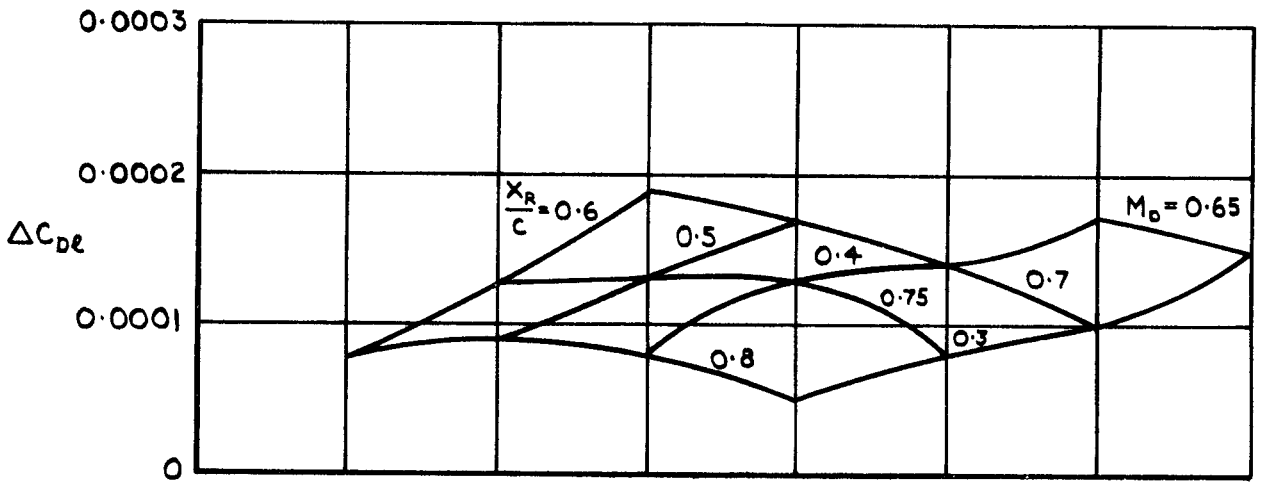

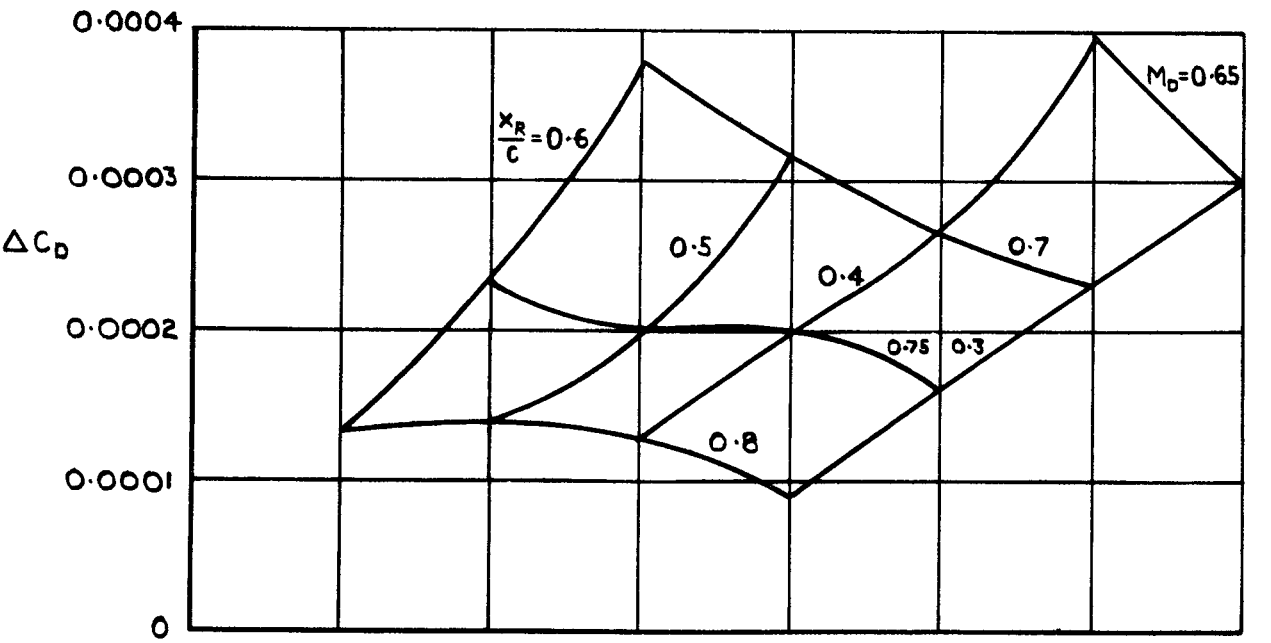

Fig. 20 Drag increments derived from correlation charts (eg Fig. 19)

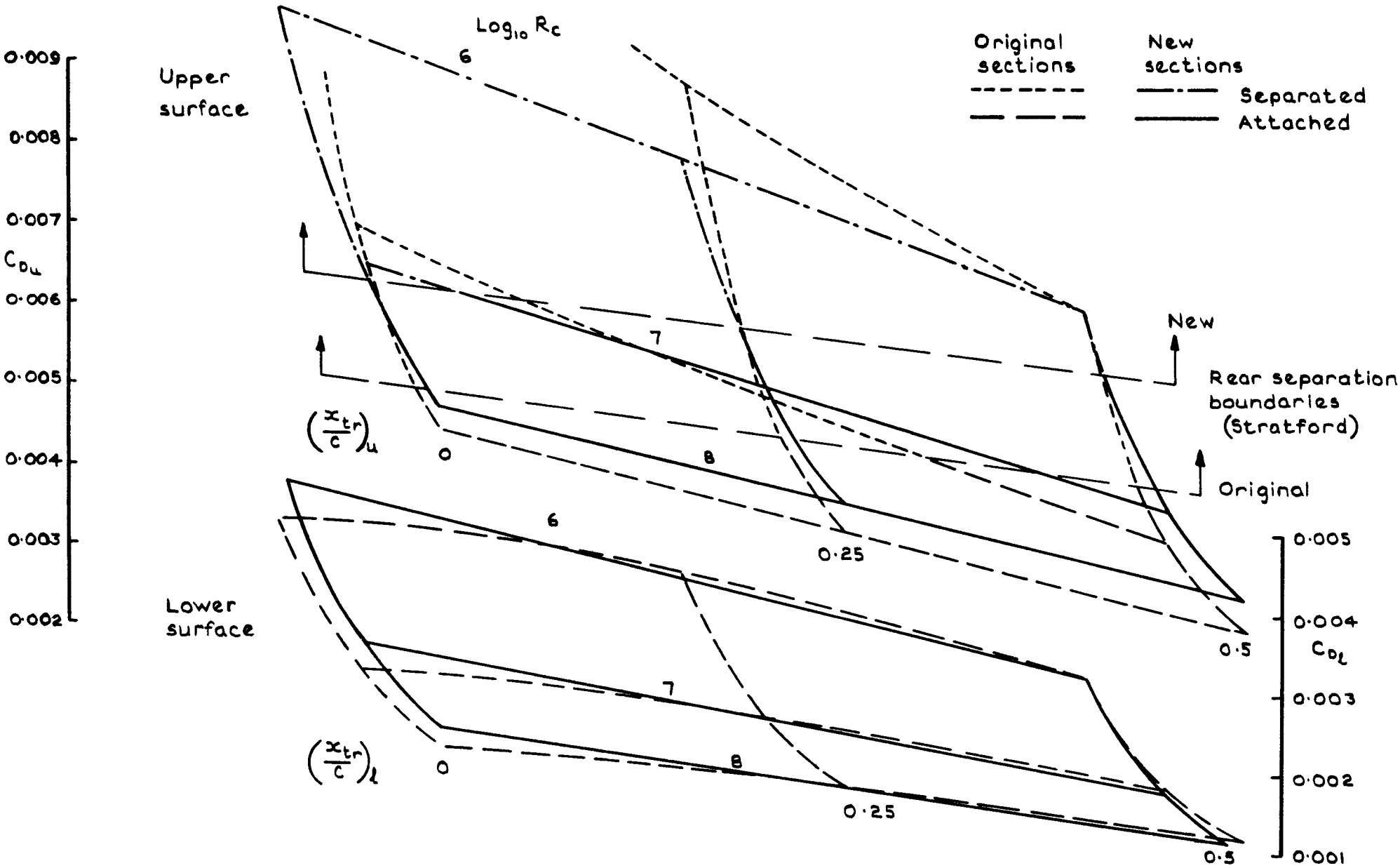

Fig. 21 Comparison of calculated profile drag for original and new aerofoil section 103 - 14 - 50 - 70 $C_L = 0 \cdot 5$

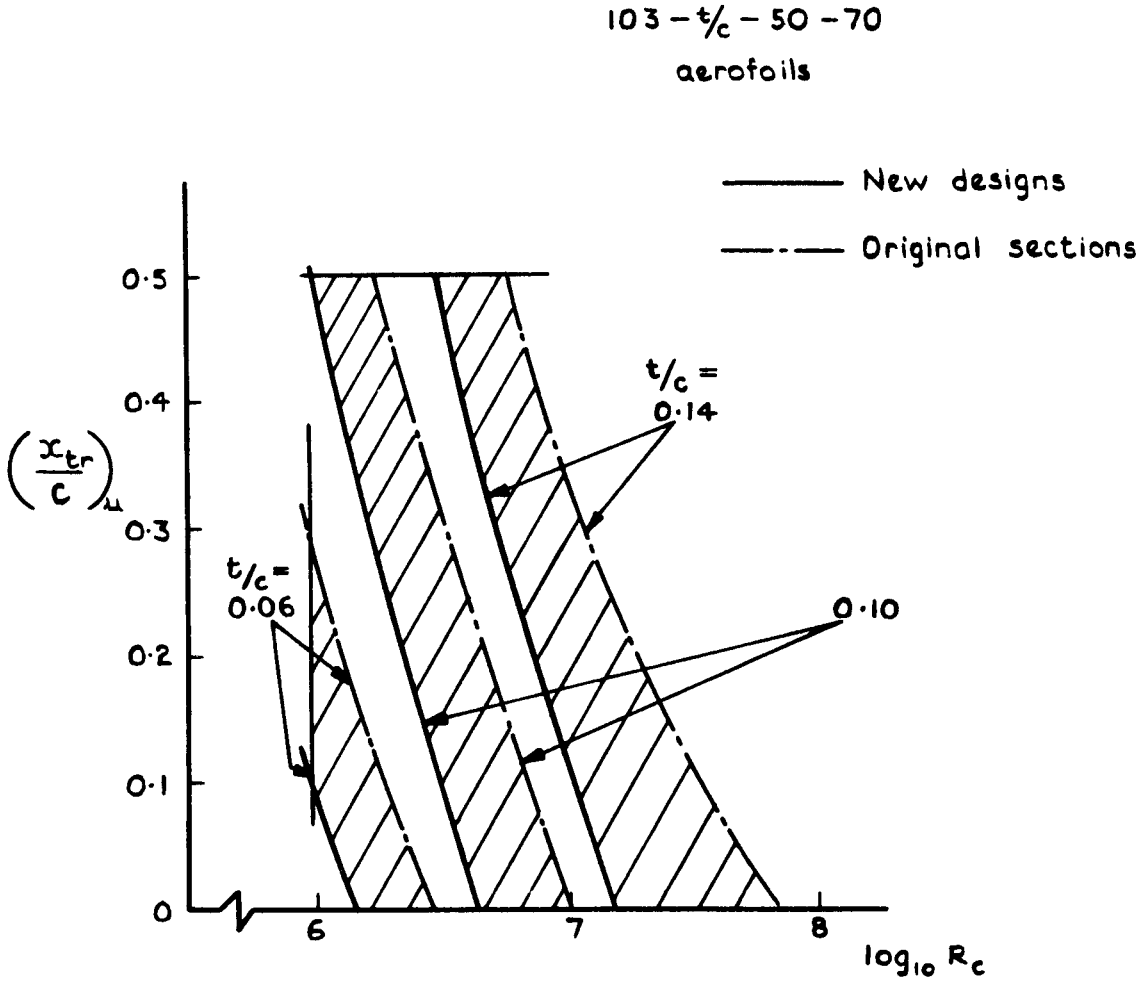

T.R. 72141

Fig. 24 Comparison of separation boundaries using Stratford's method

Printed in England for Her Majesty's Stationery Office by the Royal Aircraft Establishment, Farnborough. Dd. 289030 K4 6/75.

ARC CP No.1320
July 1972

533.692 :
533.6.048.2 :
533.6.013.12 :
532.526.5

Thompson, B. G. J.
Cosby, S. W.

THE CHARACTERISTICS OF A FAMILY OF ROOFTOP AEROFOILS DESIGNED AT THEIR DRAG-RISE CONDITION IN VISCOUS, COMPRESSIBLE FLOW.
Part 1: Design condition

Twenty-eight members of the original family of aerofoils, presented in TDM 67010, have been redesigned using an inverse method which takes account of the major influence of the boundary layer and wake on the pressure distribution. The more accurate compressibility law devised by Wilby and Lock is used. Hodges results suggesting that the published family has an overoptimistic performance are confirmed. The new sections have design lift coefficients which are usually lower than the original values by amounts up to 10%. Their drag coefficients are higher by 0.0001 to 0.0004 but they have a wider range of attached flow in conditions of practical interest, according to Stratford's method, because of more realistic trailing edge pressures.

(Over)

ARC CP No.1320
July 1972

533.692 :
533.6.048.2 :
533.6.013.12 :
532.526.5

Thompson, B. G. J.
Cosby, S. W.

THE CHARACTERISTICS OF A FAMILY OF ROOFTOP AEROFOILS DESIGNED AT THEIR DRAG-RISE CONDITION IN VISCOUS, COMPRESSIBLE FLOW.
Part 1: Design condition

Twenty-eight members of the original family of aerofoils, presented in TDM 67010, have been redesigned using an inverse method which takes account of the major influence of the boundary layer and wake on the pressure distribution. The more accurate compressibility law devised by Wilby and Lock is used. Hodges results suggesting that the published family has an overoptimistic performance are confirmed. The new sections have design lift coefficients which are usually lower than the original values by amounts up to 10%. Their drag coefficients are higher by 0.0001 to 0.0004 but they have a wider range of attached flow in conditions of practical interest, according to Stratford's method, because of more realistic trailing edge pressures.

(Over)

These abstract cards are inserted in Technical Reports for the convenience of Librarians and others who need to maintain an Information Index.

Cut here

ARC CP No.1320
July 1972

533.692 :
533.6.048.2 :
533.6.013.12 :
532.526.5

Thompson, B. G. J.
Cosby, S. W.

THE CHARACTERISTICS OF A FAMILY OF ROOFTOP AEROFOILS DESIGNED AT THEIR DRAG-RISE CONDITION IN VISCOUS, COMPRESSIBLE FLOW.
Part 1: Design condition

Twenty-eight members of the original family of aerofoils, presented in TDM 67010, have been redesigned using an inverse method which takes account of the major influence of the boundary layer and wake on the pressure distribution. The more accurate compressibility law devised by Wilby and Lock is used. Hodges results suggesting that the published family has an overoptimistic performance are confirmed. The new sections have design lift coefficients which are usually lower than the original values by amounts up to 10%. Their drag coefficients are higher by 0.0001 to 0.0004 but they have a wider range of attached flow in conditions of practical interest, according to Stratford's method, because of more realistic trailing edge pressures.

(Over)

Cut here

DETACHABLE ABSTRACT CARDS

DETACHABLE ABSTRACT CARDS

The drag values, separation boundaries and drag-rise boundaries are presented in Ref.12, together with tabulation of ordinates and design pressure distributions for the complete series of redesigned aerofoils. The present Report considers mainly the 50% rooftop sections as typical examples and discusses the basis upon which the new designs were obtained.

The drag values, separation boundaries and drag-rise boundaries are presented in Ref.12, together with tabulation of ordinates and design pressure distributions for the complete series of redesigned aerofoils. The present Report considers mainly the 50% rooftop sections as typical examples and discusses the basis upon which the new designs were obtained.

The drag values, separation boundaries and drag-rise boundaries are presented in Ref.12, together with tabulation of ordinates and design pressure distributions for the complete series of redesigned aerofoils. The present Report considers mainly the 50% rooftop sections as typical examples and discusses the basis upon which the new designs were obtained.

The drag values, separation boundaries and drag-rise boundaries are presented in Ref.12, together with tabulation of ordinates and design pressure distributions for the complete series of redesigned aerofoils. The present Report considers mainly the 50% rooftop sections as typical examples and discusses the basis upon which the new designs were obtained.

C.P. No. 1320

1975

Published by
HER MAJESTY'S STATIONERY OFFICE

Government Bookshops
49 High Holborn, London WC1V 6HB
13a Castle Street, Edinburgh EH2 3AR
41 The Hayes, Cardiff CF1 1JW
Brazennose Street, Manchester M60 8AS
Southey House, Wine Street, Bristol BS1 2BQ
258 Broad Street, Birmingham B1 2HE
80 Chichester Street, Belfast BT1 4JY
Government Publications are also available through booksellers

C.P. No. 1320

ISBN 011 470930 0